1-1-2002

Practical implementation of an Unequal Three-Tone Signal for determining AM to AM and AM to PM conversion factor in RF low noise amplifiers operating at a frequency of 1 GHz

Hasib Jahangir
Iowa State University

Practical implementation of an Unequal Three-Tone Signal for determining AM to AM and AM to PM conversion factor in RF low noise amplifiers operating at a frequency of 1 GHz

by

Hasib Jahangir

A thesis submitted to the graduate faculty

in partial fulfillment of the requirements for the degree of

MASTER OF SCIENCE

Major: Electrical Engineering

Program of Study Committee:
Robert J. Weber, Major Professor
David T. Stephenson
Fred Wright

Iowa State University

Ames, IA

2002

Graduate College
Iowa State University

This is to certify that the master's thesis of

Hasib Jahangir

has met the thesis requirements of Iowa State University

Signatures have been redacted for privacy

TABLE OF CONTENTS

CHAPTER 1. INTRODUCTION

The last few years has seen a remarkable growth and demand in the area of personal and wireless communication systems. Large numbers of mobile phone cell sites operating with different communication standards has been implemented through out the world. As a result, the need for optimizing the circuits involved in any cellular base-station has increased. Efficient bandwidth utilization and power efficiencies are the most important aspects of any base-station transmitter [7]. Multilevel digital modulation techniques such as 16 QAM or 256 QAM in conjunction with different multiple access techniques such as TDMA or CDMA are utilized to achieve spectrum efficiency. Use of these methods results in fluctuations of the transmitted signal's envelope which are very sensitive to nonlinearities in communication systems. Solid-state power amplifiers (SSPA) used in base-station transmitters are the main cause of these nonlinearities [7]. The power amplifier (PA) is the component of an RF system that takes the signal to be transmitted and amplifies it to the necessary level needed to drive the antenna for a particular power output level. In most wireless communication systems, the PA is the largest power consumer, usually because the amount of power that needs to be sent to the antenna (the power output) is itself very large. This does not include the total power that is consumed within the PA, just the amount that is required to drive the antenna. The total power consumed by the PA is necessarily greater than the power output. As a result, the performances of the PA regarding its power consumption and linearity directly affect the transmission capacity of the communication system. In modern communication systems where microwave low noise amplifiers and systems are utilized,

minimization of amplitude modulation to phase modulation (AM/PM) conversion distortion becomes very critical. AM to PM conversion is a form of distortion associated with the nonlinearities inherent in solid-state transistor components of microwave amplifiers. In practice, measuring the power efficiency of the PA is easier than the characterization of its nonlinear distortions. AM to PM conversion mainly increases noise in communication systems which results in a distorted signal, loss of important information in the signal or higher average bit error rate at the receiving end of the system. AM/PM conversion factor is defined as the change in phase angle of the RF voltage at the output of a microwave amplifier due to amplitude variations in the input signal [9]. It is expressed in degrees/decibel (°/dB). More importantly, it should be defined at a specific power level. When microwave amplifiers are utilized close to their power output limits, linear measurement techniques fail to characterize its final performance. In this thesis, a practical implementation of a new technique for characterizing AM to PM distortion of microwave PA circuits using only power measurements is discussed. The laboratory implementation method and measurement procedure of this technique is based on the IEEE short paper by *F.M. Ghannouchi, H. Wakana, and M. Tanaka* [8]. This technique is based on using an unequal 3-tone test signal having both amplitude and phase modulation to drive the nonlinear device-under-test (DUT). In our case, the DUT is a *Class A or Class C* power amplifier operating at a frequency of 1 GHz. Measuring the power levels of the unequal three tone test signal (UTTS) at the input and output of the DUT allows the calculation of the AM/PM conversion coefficient of the amplifier at the chosen frequency and power level.

Architecture of RF System

The basic structure of an RF transceiver system for personal communications is shown in Figure 1. On the transmitter side of the system, the basic operations are as follows. After encoding the digital data (i.e. i_k & q_k bit streams), the independent I and Q channels of data (i.e. baseband waveforms) are combined by some form of quadrature modulator, and the resulting combination is mixed up to the RF carrier frequency (or the two steps could be combined into one block as in Figure 1). Then, after some filtering (not shown), the signal drives the power amplifier, which drives the antenna. The antenna radiates the signal into the air, and the transmission is complete.

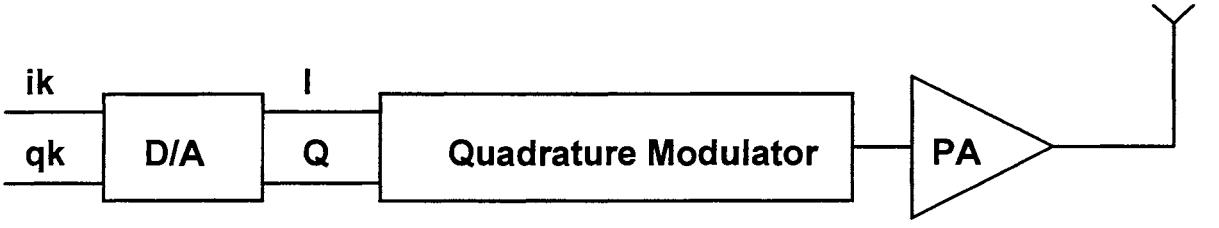

(a) Common Transmitter Architecture

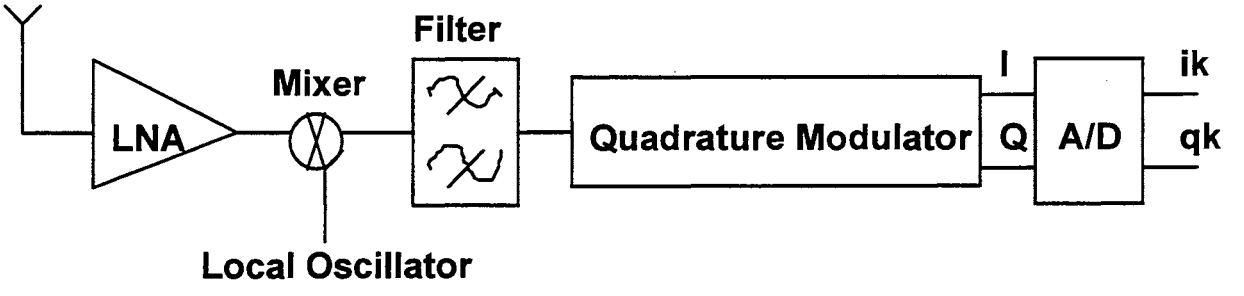

(b) Common Receiver Architecture

Fig. 1. Basic RF Transceiver System

The receiver side is simply the inverse with a slightly different component configuration. The signal received by the antenna is filtered to select the RF band of interest, after which it is fed into a Low Noise Amplifier (LNA). The signal is then either mixed directly down to baseband and filtered, in the case of a direct conversion or homodyne receiver, or mixed to one or more intermediate frequencies (IF) and filtered (Figure 1), in the case of a heterodyne or super-heterodyne receiver. Usually the last mixing stage which is the quadrature demodulator will separate the signal into its I and Q components. Once at baseband, the signal will be converted to a digital form and then processed to extract information. The RF amplifier exists at both the transmitter and receiver section of the system where AM-AM and AM-PM conversion takes place and thus affects the signal quality.

CHAPTER 2. PROBLEM DEFINITION

A memoryless PA operating in the nonlinear region when excited by a microwave signal having a certain frequency bandwidth centered around a carrier frequency of f = 1 GHz can be characterized by its AM-AM compression and AM-PM conversion curves [8]. In our case, the RF input should be a voltage signal containing both amplitude (AM) and phase (PM) modulation. Basic input and output RF signals for any test case involving a low noise power amplifier (LNA) is described below.

In the time domain, the RF input signal is of the form : $V_{in}(t) = A(t)cos[\omega t + \theta(t)]$ (1)

The RF output signal is of the form : $V_{out}(t) = G\{A(t)\}cos[\omega t + \theta(t) + \Psi\{A(t)\}]$ (2)

In the above equations, $A(t)$ = Gain Factor

$\theta(t)$ = Phase Factor

$G\{A(t)\}$ = AM-AM Compression curve

$\Psi\{A(t)\}$ = AM-PM Conversion curve

In this formulation, it is assumed that the RF signal bandwidth $2\Delta\omega$ is centered on the carrier frequency ω such that $\Delta\omega$ is much less than the carrier itself. We also assumed that that the PA has a flat complex gain over the $2\Delta\omega$ frequency bandwidth centered around ω. In order to generate an RF input to the PA having both AM and PM modulation, a superposition of a low-index sinusoidal AM signal and a low-phase deviation sinusoidal PM signal was obtained using two different signal generators in the lab. If the input RF signal is a superposition of a low-index sinusoidal AM signal and a low-phase deviation sinusoidal PM

signal, equation (1) takes the following form :

$$V_{in}(t) = A_o[1 + \alpha\cos\{\Delta\omega t\}]\cos[\omega t + \beta\sin\{\Delta\omega t\} + \theta_o] \quad (3)$$

In equation (5), α = Amplitude Modulation Index of the AM signal

β = Phase Modulation Index of the PM signal

A_o = Average Amplitude of the AM signal

θ_o = Average Phase of the PM signal

Assuming small variations of PA phase-shift with power level, it has been demonstrated that the PA phase-shift variation is proportional to the input power level. As a result, this variation in phase-shift is would be proportional to the square of the input signal envelope [8]. Applying the signal in equation (3) at the input of the PA would produce an output signal of the form given below :

$$V_{out}(t) = GA_o[1 + \alpha\{(1-c)\cos(\Delta\omega t)\}]\cos[\omega t + \theta_o + \Delta\theta + \beta\sin(\Delta\omega t) + k_p\alpha\cos(\Delta\omega t)] \quad (4)$$

In the frequency domain, both the input and output RF signals can be analyzed as a superposition of three unequal sinusoidal tones comprised of a carrier at the center and two unequal sidebands due to combined effect of the AM and PM in the signals.

In equation (4), G = Operating Voltage Gain of the PA

$$c = 1 - \frac{\frac{\Delta Vout}{Vout}}{\frac{\Delta Vin}{Vin}} \text{ is the AM-AM compression factor of the PA} \quad (5)$$

When the PA is operating in the linear region, $c = 0$ and when the PA is completely in saturation $c = 1$.

$$k_p = \frac{\Delta\theta}{\alpha} \text{ is the AM-PM conversion coefficient of the PA} \quad (6)$$

$\Delta\theta$ = Peak phase change due to AM-PM conversion

The block diagram of the PA with its corresponding spectrum of the input and output RF signals having both AM and PM is shown in Figure 2.

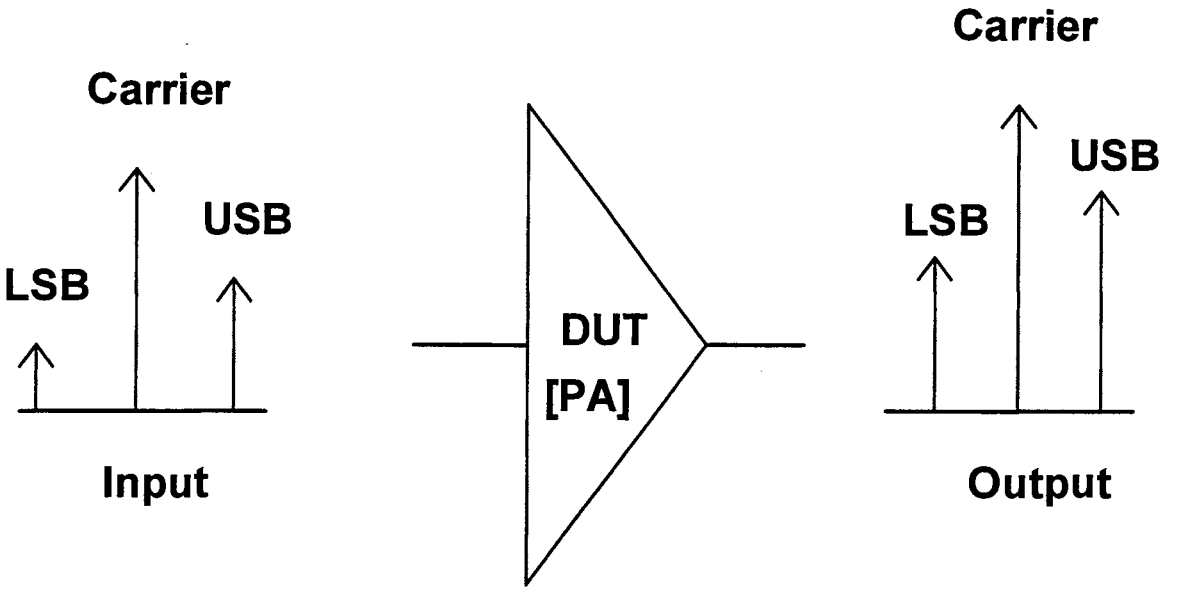

Fig. 2. PA Block Diagram with I/O RF Signal Spectrum

Location of the LSB = Lower Sideband is at frequency ω-$\Delta\omega$.

Location of the USB = Upper Sideband is at frequency ω+$\Delta\omega$.

It is important to note that the relative difference in power level between the upper and the lower sideband at the input is essentially different than the power level difference at the output of the PA. This is due to the nonlinear characteristics inherent in the solid state transistor used to build the PA. As a result, an extra AM due to AM-AM compression and an extra PM due to AM-PM conversion affect the sidebands at the output . In summary, the

parameters G, c, and k_p characterizes the PA and the parameters A_o, α, β characterizes the input and output RF signal. To characterize the AM-AM and AM-PM distortions of the PA using the UTTS method, our goal is to solve the equations to calculate G, c, and k_p as functions of the amplitudes at the input as well as at the output of the PA [8]. Since only power measurements at the input and the output are of interest, it was found suitable to use a voltage signal for the characterization of the PA. The formulation of equation (3) and the discussion in this part of the thesis is based on the IEEE short paper on the UTTS method by F. M. Ghannouchi, H. Wakana and M. Tanaka [8].

CHAPTER 3. ANALYTICAL APPROACH

As mentioned earlier, the RF input to the power amplifier contains both a low index amplitude modulation and a low phase deviation phase modulated carrier signal. The spectrum of the input signal with AM only in equation (3) can be expressed using trigonometric identities as follows :

$$V_{in\text{-}AM}(t) = \{A_o/2\}\cos[\omega t] + \{\alpha A_o/2\}\cos[\{\omega+\Delta\omega\}t] + \{\alpha A_o/2\}\cos[\{\omega-\Delta\omega\}t] \quad (7)$$

Since it is a low index AM signal, the upper and lower sidebands remain in phase. Similarly, the spectrum of the input signal with PM only in equation (5) can be expressed as follows :

$$V_{in\text{-}PM}(t) \cong \{A_o/2\}\cos[\omega t] + \{\beta A_o/2\}\cos[\{\omega+\Delta\omega\}t] - \{\beta A_o/2\}\cos[\{\omega-\Delta\omega\}t] \quad (8)$$

But unlike the AM part of the input signal, the upper and lower sidebands of the PM signal are out of phase. For both AM and PM components of the input signal, the carrier amplitude is $A_o/2$. As a result, the carrier amplitude of the total input signal becomes A_o due to constructive interference of AM and PM carrier components. Both the α and β are kept very small and $\alpha \geq \beta$ in order to make sure that the energy in higher order side-bands are very small compared to the first order side-bands. Superposition of the signals in equation (7) and (8) results in a total input signal having a spectrum as follows :

$$V_{in}(t) \cong V_{AM\text{-}in}(t) + V_{PM\text{-}in}(t)$$

$$= \{A_o\}\cos[\omega t] + \{A_{USB\text{-}in}/2\}\cos[\{\omega+\Delta\omega\}t] - \{A_{LSB\text{-}in}/2\}\cos[\{\omega-\Delta\omega\}t] \quad (9a)$$

In equation (9a), $A_{USB\text{-}in}$ = Input Amplitude of the upper or right hand sideband.

$A_{LSB\text{-}in}$ = Input Amplitude of the lower or left hand sideband.

So, $V_{in}(t) \cong \{A_o\}\cos[\omega t] + \{(\alpha+\beta)A_o/2\}\cos[\{\omega+\Delta\omega\}t] - \{(\alpha-\beta)A_o/2\}\cos[\{\omega-\Delta\omega\}t]$ (9b)

By measuring the power levels of the upper and lower sidebands of the input signal and subsequently converting them to R.M.S voltages, the AM and PM index can be calculated as follows : $\alpha = \{A_{USB\text{-}in} + A_{LSB\text{-}in}\}/A_o$ (10a)

$$\beta = \{A_{USB\text{-}in} - A_{LSB\text{-}in}\}/A_o \quad (10b)$$

As the input signal in equation (9b) is applied to the input of the DUT, it goes through amplification, AM-AM compression and AM-PM conversion. As mentioned earlier, the upper and lower sidebands of the input signal are equally spaced by an amount of $\Delta\omega$ from the carrier component. As a result, the composite signal at the amplifier input (Class A or Class C) is an RF signal with center frequency at ω with amplitude and phase modulation at a rate of $\Delta\omega$. It should be noted that there will be negligible or zero compression when the amplifier is operating purely in the linear region. When the amplifier is completely saturated, the compression becomes 100 percent and it operates as a limiter [8]. When the amplifier is driven into its nonlinear region of operation, the AM sideband components of the RF input get compressed due to AM-AM compression at the output and each of these sideband components get multiplied by a factor of $(1\text{-}c)$. Extra PM sidebands are introduced in the output signal spectrum due to AM-PM conversion. The original PM sidebands due to phase modulation in the RF input remain unaffected by the compression. The newly generated PM sidebands due to AM-PM conversion are out of phase by 90 degree from the original AM sidebands at the output [8]. The resultant upper and lower sidebands in the output spectrum are calculated using vector addition. The vector diagram for the addition of amplified AM and PM sidebands (which are part of the output due to a RF input) and the newly generated extra PM sidebands are shown in Figure 3 on the next page.

(a) Upper or Right Hand Sideband @ Output

(b) Lower or Left Hand Sideband @ Output

Fig 3. Vector Addition Diagram for Sidebands at the PA Output

In the diagram (a), $GA_o\beta/2$ = Original PM Sideband (Upper) = 1U

$Gk_pA_o\alpha/2$ = New PM Sideband due to AM-PM (Upper) = 3U

$GA_o(1-c)\alpha/2$ = AM Sideband due to AM-AM Compression (Upper) = 2U

$A_{USB\text{-}out}$ = Resultant Upper Sideband at the Amplifier Output = 4U

In the diagram (b), $GA_o\beta/2$ = Original PM Sideband (Upper) = 2L

$Gk_pA_o\alpha/2$ = New PM Sideband due to AM-PM (Upper) = 3L

$GA_o(1-c)\alpha/2$ = AM Sideband due to AM-AM Compression (Upper) = 1L

$A_{LSB\text{-}out}$ = Resultant Upper Sideband at the Amplifier Output = 4L

It should be noted that the two PM sidebands (original & newly generated) are out of phase. According to Figure 3, the result of the vector addition of the AM and PM sideband components yields the following mathematical expressions :

$$(A_{USB\text{-}out})^2 = G^2\,[(1-c)A_o\alpha/2 + A_o\beta/2]^2 + [Gk_pA_o\alpha/2]^2 \qquad (11a)$$

$$(A_{LSB\text{-}out})^2 = G^2\,[(1-c)A_o\alpha/2 - A_o\beta/2]^2 + [Gk_pA_o\alpha/2]^2 \qquad (11b)$$

In the above equations, $A_{USB\text{-}out}$ = Output Amplitude of the upper or right hand sideband.

$A_{LSB\text{-}out}$ = Output Amplitude of the lower or left hand sideband.

If we substitute the expressions for AM and PM modulation index from equation (10a) and (10b) and use mathematical simplification, equation (11a) and (11b) can be written as follows in the form of equations of two circles with different radii [8].

$$(R_1)^2 = (c-x_1)^2 + (k_p)^2 \tag{12a}$$

$$(R_2)^2 = (c-x_2)^2 + (k_p)^2 \tag{12b}$$

In the above equations, R_1 = Radius of the circle representing the USB measurements.

$$= 2A_{USB\text{-}out}/[G(A_{USB\text{-}in} + A_{LSB\text{-}in})] \tag{13a}$$

R_2 = Radius of the circle representing the LSB measurements.

$$= 2A_{LSB\text{-}out}/[G(A_{USB\text{-}in} + A_{LSB\text{-}in})] \tag{13b}$$

x_1 = Center of the circle representing the USB measurements.

$$= 2A_{USB\text{-}in}/(A_{USB\text{-}in} + A_{LSB\text{-}in}) \tag{13c}$$

x_2 = Center of the circle representing the LSB measurements.

$$= 2A_{LSB\text{-}in}/(A_{USB\text{-}in} + A_{LSB\text{-}in}) \tag{13d}$$

G = Operating voltage gain of the DUT.

$$= A_{o\text{-}out}/A_o \tag{13e}$$

In our experimentation, the upper sideband always has a greater magnitude than the lower sideband which in fact is confirmed by the vector diagram in Figure 3. As a result, $R_1 > R_2$ and $x_1 > x_2$. Substituting equation (12a) into equation (12b) or vice-versa, the closed form expressions of the AM-AM compression factor and AM-PM conversion co-efficient are as follows :

$$c = [(R_2)^2 - (R_1)^2 + (x_1 + x_2)(x_1 - x_2)]/[2(x_1 - x_2)] \tag{14a}$$

$$k_p = \pm[(R_1)^2 - (c - x_1)^2]^{1/2} \tag{14b}$$

Caution must be exercised while measuring the AM-PM conversion factor since it can be both positive and negative according to equation (14b). Figure 4 illustrates the graphical solution of the UTTS method.

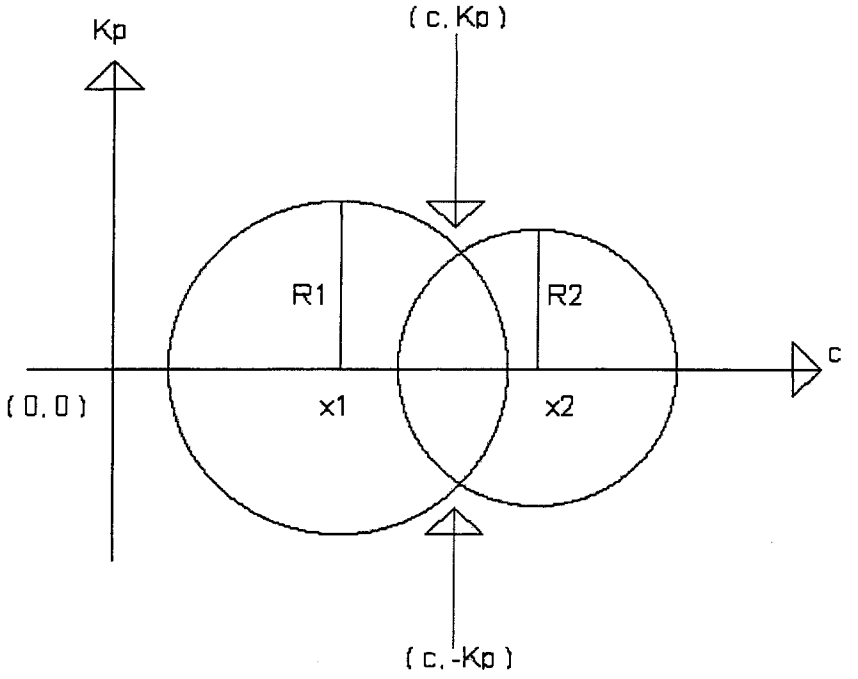

Fig 4. Graphical Solution of the UTTS Method

For each input power level at a specific carrier frequency ω, a unique set of circles were obtained. The common intersection point of these two circles gives c and k_p provided we know beforehand if k_p is negative or positive. For both Class A and Class C power amplifiers, measured data showed R_1 to be always greater than R_2. For test cases involving different PAs, the result could be other way around i.e. $R_2 > R_1$. Using a *HP 8753C* network

analyzer, amplitude and phase variation of the DUT with frequency at different power levels can be obtained. In our case the phase change with frequency for a Class A and a Class C amplifier exhibited a positive slope. This confirms the fact that the AM-PM conversion factor in our experimental case would be positive. Also obvious from the mathematical formulation of the problem is that any change in the gain of the DUT will affect the carrier and both sidebands. As a result, the relative amplitudes of the sidebands relative to the carrier will remain unchanged. Consequently, DUTs with different gain operating at some specific power level will produce similar c and k_p values [8]. During experimentation, very low level input drive signals must be used with caution. Since at very low input level, the LSB measurements would yield a R_2 value very low compared to R_1. This will result in two marginally intersecting circles that will result in inaccurate AM-AM compression and AM-PM conversion factors. In a practical implementation, an amplifier will have nonzero but negligible compression in the linear region of operation. Taking this into consideration, an error will occur in our calculation of the AM-PM conversion factor. To rectify this, $c = 0$ was used for most of the linear region in order to calculate k_p. Before doing any power measurements, it was verified using *Spice* simulation that the DUT (PA) is memoryless. This means that the PA biasing circuit has a time constant, τ which is very large compared to the modulation frequency bandwidth $2\Delta\omega$ [7]. To ensure that the UTTS method is valid, both AM and PM modulation was applied to the input RF signal. In doing this the AM modulation index α was set at a higher value than the PM modulation index β. If $\alpha = 0$ or $\beta = 0$ were used, equations (11a) and (11b) would become one with two unknowns which would lead to an infinite number of solutions with inaccurate values for c and k_p. Using

$\alpha = \beta$, would produce an input signal with only the upper sideband since $A_{LSB\text{-}in}$ becomes zero in this configuration. As a result, the circle in equation (12b) will have a center at (0,0) which will effectively make the input an unbalanced two-tone signal (UB2T) [8]. The theoretical analysis of the UTTS method described in this part of the thesis is based on the IEEE short paper by F. M. Ghannouchi, H. Wakana and M. Tanaka [8].

CHAPTER 4. PA DESIGN AND IMPLEMENTATION

In any communication system designed to transmit information between two points, many factors must be considered in the design phase of the system for error free transfer of data. The whole system needs to be broken down into discrete sub-systems and each sub-system must be implemented according to system requirements. A reliable physical media or carrier must be present which will carry the signal from one point to the other without distorting it. After the signal is transmitted by the transmitter in a coded form, it needs to be amplified at an appropriate level such that the effects of the medium in which the signal is transmitted do not prevent the signal from being received nor prevent the signal from being misinterpreted at the receiver end. This particular device is the Power Amplifier or PA. During transmission, the output of the signal is usually connected to a load such as an antenna or real circuit element. Because the power level required for reliable transmission of the signal is usually high, a lot of power is consumed in the PA. As long as the transmitted signal contains adequate power, the power consumed by the PA is not critical for many applications. But in energy critical communication applications, power consumption by all sub-systems hence the PA must be minimized in order for the available power to be utilized for longest possible time duration. In that case, the PA must consume as much power as must be transmitted.

Power Amplifier Efficiency

Ideally, a good PA would consume only the power that needs to be transmitted since it's the PA that drives the antenna with required output power. As a result, the ratio of the power

transmitted to the power consumed by the PA becomes unity. This measure of a power amplifiers performance is called the efficiency. In general,

$$Efficiency,\ \eta = P_{transmitted} / P_{consumed} \quad (15a)$$

Where, $P_{transmitted}$ = Power delivered to the load or transmitted.

$P_{consumed}$ = Power consumed by the PA.

In literature, three types of amplifier efficiency are used by system designers as follows :

$$\text{Device Efficiency, } \eta_{Device} = P_{RF\text{-}OUT} / P_{DC} \quad (15b)$$

Where, $P_{RF\text{-}OUT}$ = Power delivered to the load at a particular RF frequency.

P_{DC} = Power supplied by the DC power supply to the PA.

$$\text{Power Added Efficiency, } \eta_{pae} = (P_{RF\text{-}OUT} - P_{RF\text{-}IN}) / P_{DC} \quad (15c)$$

Where, $P_{RF\text{-}OUT}$ = Power delivered to the load at a particular RF frequency.

$P_{RF\text{-}IN}$ = Power required to drive the PA at a particular RF frequency.

P_{DC} = Power supplied by the DC power supply to the PA.

$$\text{Overall Efficiency, } \eta_{overall} = P_{RF\text{-}OUT} / (P_{DC} + P_{RF\text{-}IN}) \quad (15d)$$

P_{DC} is also called the device circuit dc input power.

The power added efficiency is the most commonly used metric in the industry. In fact, the *pae* and the overall efficiency are important in measuring the true power efficiency of a power amplifier. This is due to the fact that calculations of both efficiencies take the input RF power into consideration. Besides, the input drive level is also an important factor in determination of the amplifier gain which eventually decreases once the amplifier enters the nonlinear region of its operation. In this way, one can compare the performance of different PAs with similar device efficiency but different power gains. It should be mentioned that the

PA with more power gain will provide better power efficiency since less power is needed to excite the PA at the desired RF frequency. In an ideal case, the overall efficiency would approach one, as the power delivered to the load would be identically the same as the power taken from the supply. Then, no power would be consumed in the amplifier, or the transistors and other external circuitry, which constitute the PA. In the realm of RF spectrum, especially in the gigahertz range, power amplifier efficiencies will not be 100%. In order to amplify the signal, some power must be consumed by the transistor and other circuit elements of the PA. In many high frequency systems, the PA including the driver stage must amplify the signal as well as drive the output load. While amplifying a signal, some power is consumed in the PA. To amplify a signal efficiently, there should be little or no power at all consumed in the PA sub-system.

Power Amplifier Types

In practice, different types of configuration are available in which an application specific power amplifier can be implemented. These PAs are used when the efficiency and output power of the amplifying sub-circuit are considered critical for overall system performance. Power amplifiers can be linear or nonlinear according to the input and output terminal characteristics. In PA terminology, a linear power amplifier exhibits a linear relationship between its input and output whereas a nonlinear relationship exists between the input and output of a nonlinear PA. The transistor in a PA subsystem might switch between cutoff and saturation but the total PA block might still be linear. This behavior is clearly visible in a Class B power amplifier configured in a Push-Pull Transformer-Coupled circuit [4]. In this case, two transistors are driven 180° out of phase so that each is active for half of the signal

cycle and cut off during the other half. Neither device produces an amplified replica of the input signal. The input signal is split, amplified efficiently and then reassembled at the output [4]. In general, we assume that for every part of an input signal cycle (AC Signal), there is an output from the amplifier. However, this is not always the case as described above. Since the transistor might be off for some portion of the input cycle. Depending on the application, it is often desirable to make the transistor in the PA device conduct for only a portion of the input signal. The portion of the input for which there is an output determines the power amplifier class. There are different types of power amplifiers based on their classes of operation such as Class A, B, AB, C, D, E, F, G, H, and S [4]. In this thesis report, only Class A and Class C power amplifiers are discussed since they are the focus of this research.

Class A Amplifier

Class A amplifier is the simplest and basic form of power amplifier. In Class A operation, the transistor remains in its active region for the entire input signal cycle and thus always conducts current. This kind of amplifier is biased in such a way that variations in the input signal polarities occur within the limits of cutoff and saturation. In an NPN transistor, if the base becomes more negative with respect to the emitter, electrons will be repelled at the PN junction and almost no minority electrons will be available in the base region. As a result, no collector-current will flow and thus creating a condition called CUTOFF. If the base becomes so positive with respect to the emitter, changes in the signal cycle are not reflected in the collector-current. This situation is called SATURATION. A biasing scheme in a Class A amplifier places the DC operating point between cutoff and saturation allowing

collector current to flow during the complete input cycle (360°). As a result, the amplifier produces an output that is an amplified replica of the input and the device conduction angle becomes 360°. Figure 5 shows a simple Class A amplifier for both PNP and NPN transistors.

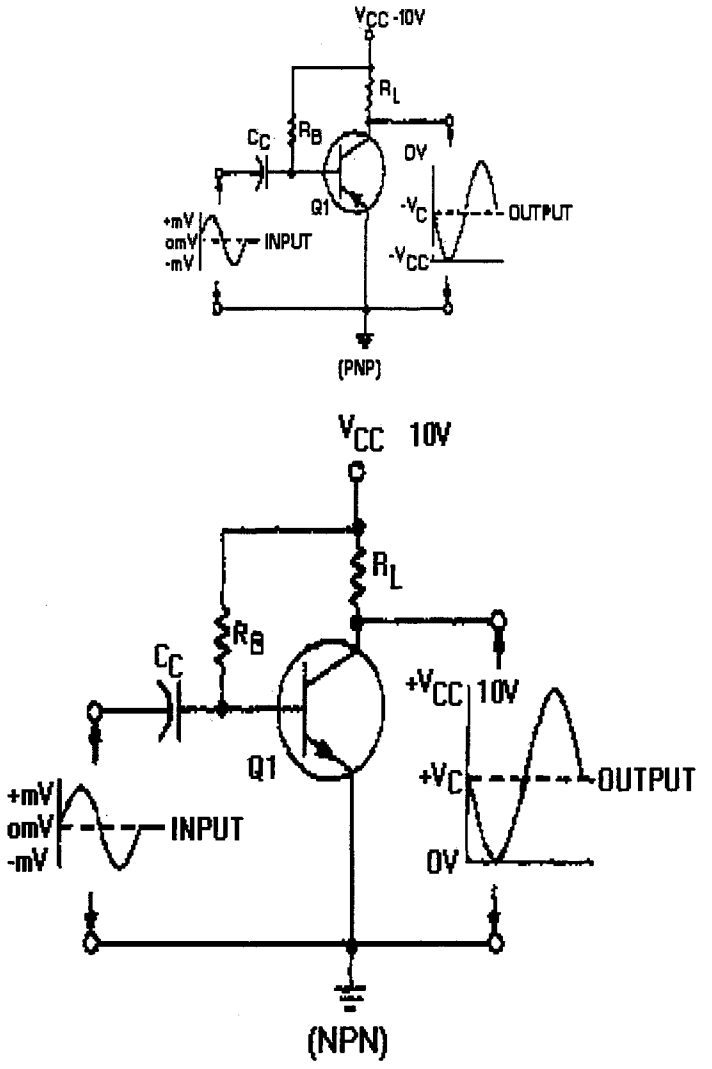

Fig 5. Basic Class A Amplifier

The transistor in Figure 5 is connected in a common-emitter configuration since the emitter is common to both input and output of the amplifier circuit. The input is 180° out of phase from the output. Since the Class A amplifier in Figure 5 can be modeled by 2-port Y parameters or by a linear equivalent Hybrid-Pi circuit due to the small signal amplitudes and linear relationship exists between the output and input, it can be called a small-signal amplifier [4]. The only problem with a Class A power amplifier is that its efficiency is limited to 50%. Since the transistor is always conducting and thus carrying current for the entire input cycle, a great deal of power is consumed compared to the power delivered to the load. Class A amplifiers are used in situations where linearity requirements are very stringent. Common applications of Class A RF amplifiers are low level driver amplifiers where a relatively small portion of the total transmitted power is consumed by the amplifier itself [4].

Class C Amplifier

A Class C amplifier is used in RF applications where power efficiency of the amplification sub-system is a more critical than the amplifier input-output linearity. If the information to be transmitted is contained in something other than the amplitude of the output signal, a non-linear amplifier like Class C can be used with its efficiency optimized for the particular application. In Class C operation, the collector current flows for less than half of the input cycle. The operation of this kind of amplifier is achieved by reverse biasing the emitter-base junction. In other words, the transistor is biased just below the threshold that is V_{BE} is less than about 0.7 V. As a result, the device conduction angel becomes less than 180°. When a voltage signal (AC) is applied to the input of the transistor, a part of the positive input swing

will drive the transistor in the active region and collector current will flow in the device only for that duration of the input. As soon as the input goes negative, the transistor will be cutoff and no collector current will flow through the transistor. As a result, the output current becomes a pulsed representation of the input. Due to the pulsed nature of the output current, the input and output voltage will not exhibit a linear relationship. As a result, the output of the PA will be highly distorted when the input voltage amplitude is changing. This is the case when the input voltage is an AC signal. The effect of the Class C operation is to minimize the current through the transistor when the voltage across the device is high and minimize the voltage across the output when the current through the transistor is high. As a result, the power dissipated in the transistor is minimized. One of the most important characteristics of an ideal Class C amplifier is the fact that the transistor is thought of as a current source [4]. This means the current through the device should be independent of the voltage across the output terminals. For a BJT based Class C amplifier, this implies that the device should remain in its forward active region, that is in its high gain state. This means V_{BE} of the BJT transistor must remain greater than its $V_{CE(sat)}$ which is usually greater than 0.2 V and often greater than 2V in high voltage devices. As a result, the output swing will decrease from the supply voltage V_{cc} to V_{cc}-*0.2 V*. The voltage waveform at the output of a Class C PA is kept at the same frequency as the input by placing a tuned circuit, which will attenuate all non-fundamental frequencies generated by the device. In the case of an ideal Class C PA, the efficiency can reach as high as 100%. This could be achieved by applying an ideal voltage waveform to turn the device on for a short instant and thus have a corresponding instantaneous current to generate the needed output power. In reality, this situation is impossible. So, the efficiency of a Class C PA is usually around 60% or higher.

Power Amplifier Bias Circuit

One of the basic problems with power amplifiers is establishing and maintaining the proper values of quiescent current and voltage in the circuit. The goal of a proper dc bias network is to select an appropriate quiescent point and maintain that condition over variations in transistor parameters and ambient temperature. Variations in ambient temperature can cause changes in amplification and even distortion of the desired output signal. The proper biasing condition or DC operating point of the transistor circuit means the values of the collector current and voltage of the transistor when no AC swing is applied to the input. There are mainly two types of bias networks. They are described briefly as follows :

Passive Bias Network

Usually, this kind of bias network is built from passive circuit components such as a resistor, inductor and capacitor. For a Class A application, a resistor R_B is connected between the collector supply voltage and the base of the transistor as in Figure 5. If the transistor temperature rises for any reason, collector current will increase. As a result, the dc operating point of the amplifier changes from its desired value and thus this method is thermally unstable [3].

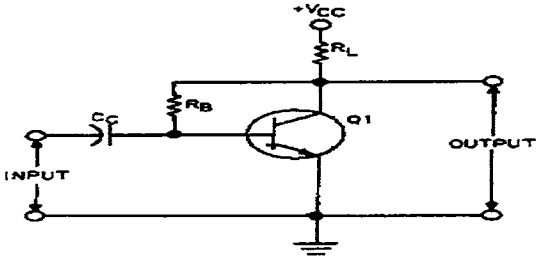

Fig 6. Alternate Bias Network for Class A PA

This method can be improved by replacing the resistor above and connecting it directly between the collector and base of the transistor (Refer to Figure 6). In this way, feedback voltage can be fed from the collector to the base to drive the transistor into forward bias region. Due to temperature increase, the collector current will increase causing the collector voltage to drop due to increased voltage in the load resistor R_L. The drop in collector voltage will be fed back to the base causing a decrease in the base current. This will eventually oppose the original increase in collector current and tend to stabilize the bias point to its original value. When the collector current decreases, the opposite happens. For moderate ambient temperature changes, this method works with good results. But amplification in the circuit is reduced somewhat. This is because the AC signals at collector and base of the transistor are opposite in polarity i.e. 180° out of phase (Refer to Figure 5). As a result, the input signal is reduced partly by the negative feedback of the collector signal. Many other resistive bias networks are possible. For lower microwave frequencies, the dc biasing network shown in Figure 7 with a bypassed emitter resistor can provide excellent stability [2].

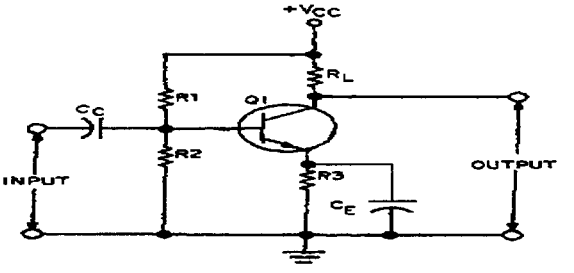

Fig 7. DC Bias Network with Bypassed Emitter Resistor

By making the C_E large enough, rapid variation in the AC swing will not change the capacitor charge and no degeneration of signal will occur.

Active Bias Network

At microwave frequencies, transistor parameters such as I_{CBO}, h_{FE} & V_{BE} are affected most and ambient temperature change is very large [2]. Moreover, bypass capacitors in parallel with emitter resistor can produce oscillations by making the input port unstable at some frequencies [2]. This is why an active bias network is the preferred choice for the operating point stability of microwave power amplifiers operating in gigahertz region. For the Class A application of this research project, a pnp BJT transistor bias network is used to stabilize the operating point of the Class A amplifier at 1 GHz. It should be mentioned that a MMBR901LT1 npn BJT transistor was used to devise the RF Class A power amplifier. The bias pnp transistor used was a 2N2907A. Figure 8 shows the complete Class A RF PA with its input & output matching circuit connected to its active bias network.

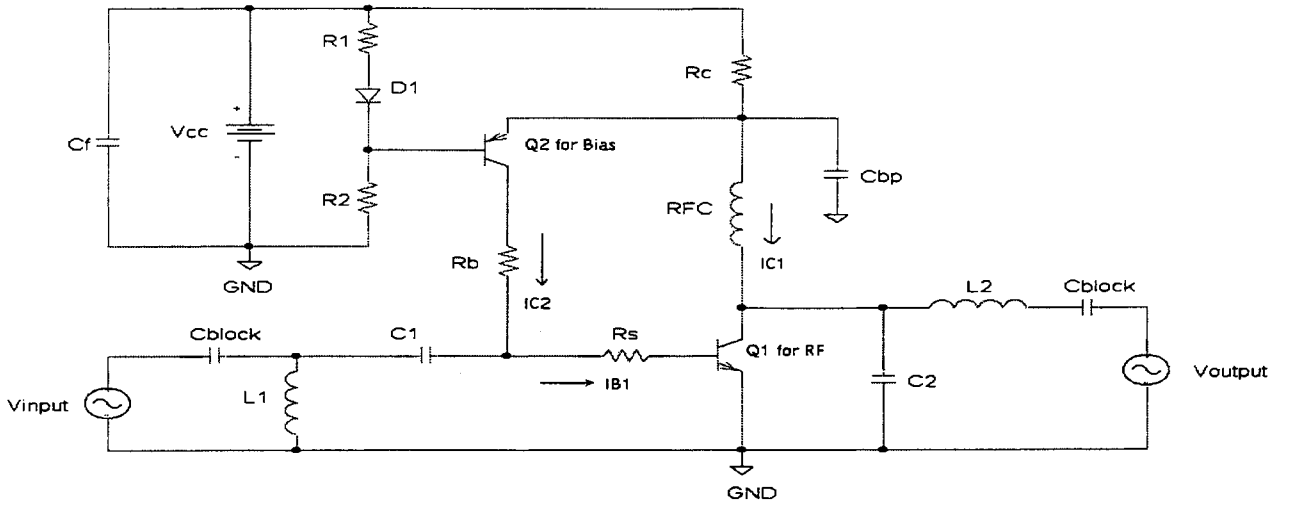

Fig 8. Class A Power Amplifier with Active Bias Network

In this Class A power amplifier circuit configuration, Q1 is the npn transistor used to amplify the RF signal. Q2 is the pnp transistor used to provide the active bias for the RF amplifier. This active bias network actually provides a negative feedback to the amplifier circuit. According to the transistor parameter specifications provided by the manufacturer, common emitter gain or β for Q1 and Q2 was chosen to be 65 and 180 respectively for theoretical calculations. A simple diode is used to track the V_{BE} of the pnp transistor. R_1 and R_2 resistors act as a voltage divider circuit. For this Class A amplifier, the bias point was set at $V_{CE1} = 10V$ and $I_{C1} = 20mA$ while the supply voltage V_{CC} is set at standard 12V. The turn-on voltage, $V_{BE1} = 0.7V$ for Q1 and for Q2, $V_{BE2} = -0.7V$. The base current for Q1 is very low since $I_{C1} = \beta_1 I_{B1}$. The collector current into Q2 is the negative of the base current into Q1 i.e. $I_{B1} = -I_{C2}$ making I_{B1} very small. The negative sign indicates the polarity of the current. As a result, I_{E2} is also very small since $I_{E2} = I_{C2} + I_{B2}$. If the collector current increases due to temperature or transistor parameter variations, increased voltage drop in R_C decreases V_{CE}. As a result, the dc bias point of the amplifier circuit is destabilized. Since a portion of the I_{C1} is fed back to Q1 through the pnp bias controller circuit, V_{BE2} will become less negative and Q2's base-emitter junction will be less forward biased. Thus values of I_{B2} and I_{C2} will decrease. As a result, I_{B1} will decrease for reasons stated earlier. Eventually, I_{C1} will decrease proportionately to its previous stable value and thus restoring the operating point of the RF amplifier to its desired value. For a decrease in I_{C1}, the opposite occurs. The mathematical calculations for choosing the resistor values (Refer to Figure 8 for all equations) are described below :

Using Kirchoff's voltage law, $V_{C1} = V_{R2} + V_{EB2}$ (16a)

$\Rightarrow V_{R2} = 10 - 0.7 = 9.3$ V since $V_{EB2} = -V_{BE2}$ and $V_{C1} = V_{CE1}$.

Using Kirchoff's voltage law, $V_{CC} = V_{CE} + I_C R_C$ (16b)

$$\Rightarrow R_C = 100\ \Omega.$$

From the voltage divider on the bias network, $V_{R2} = \{(R_2)/(R_1 + R_2)\}(V_{CC} - V_{D1})$ (16c)

$$\Rightarrow (R_2)/(R_1 + R_2) = 0.823.$$

Using resistors available in the lab, choosing $R_2 = 10$ kΩ yields $R_1 = 2.15 \approx 2.2$ kΩ.

R_b needs to be high enough to minimize the loading on the input RF circuit. It would be appropriate to keep this resistor value between 500 Ω and 1 kΩ. In this case, $R_b = 680\ \Omega$ was selected.

Using common-emitter gain, $I_{B1} = I_{C1}/\beta = 0.02/65 = 307.7\mu A$.

$$I_{B2} = I_{C2}/\beta = -I_{B1}/\beta = -1.71\mu A.$$

Blocking capacitors were connected both at input and output of the RF amplifier in order to prevent DC current flowing into instruments connected to the input and output ports of the PA. Both blocking capacitors were chosen to be 100 pF providing a sufficiently low impedance for this application. The bypass capacitor $C_{bp} = 50$ pF in parallel with the RF choke RFC is used to ground any RF signal at 1GHz frequency that might flow into the bias circuit. The RF choke is a parallel resonant inductor with a value of 110 nH. In this way, signals in the RF part of the circuit can be prevented from disrupting the DC bias circuit. In the case of a Class C amplifier, no particular bias controller circuit was used since at every input RF power level, the bias point will change. Thus, changes in the test setup and instrument controls were made manually to maintain the bias point ($I_C = 20\ mA$ & $V_{CE} = 10V$). Power levels chosen for testing the Class C amplifier were very different than those

used for Class A amplifier. It became somewhat difficult to maintain the proper bias point for the Class C amplifier.

Class A Design Process

For simplicity and ease of operation, this particular Class A power amplifier for the project was designed with its operating frequency at 1GHz. To simulate the behavior of the amplifier at the desired frequency, HP-ADS microwave circuit design software was used. The solid-state device or transistor used in this project was a MOTOROLA *mmbr901LT1*which is a surface mounted high frequency npn silicon microwave transistor. This transistor is primarily designed for use in application where high-gain with low-noise signal amplification is desired for operation up to 2.5 GHz. The schematic level simulation was based on the small signal S-Parameters available in the lab from MOTOROLA Inc. For this reason, the Class A amplifier is also a small signal amplifier. For maximum device ratings and various operational characteristics & parameters, refer to the transistor technical data sheet in Appendix B.

HP-ADS Simulation & Parameters Setup

In the HP-ADS schematic design environment, a 3-terminal 2-port DUT was selected to represent the RF transistor. Next, the S-Parameter data file was attached to the DUT so that during the simulation phase, HP-ADS can interpret the small signal characteristics to obtain various results such as stability, input-output matching conditions, gain, parasitics considerations etc. Since the final circuit was to be built on a printed circuit board (PCB), the material characteristics of the board need to be taken into consideration for realistic simulation results. The microstrip input and output lines for the amplifier module are called

Port 1 and Port 2 respectively and have a characteristic impedance of 50 Ω. Rogers, RO4003 material was used to fabricate the circuit board for both the Class A and Class C amplifier. This particular material is designed for precise high frequency performance with low attenuation. Before simulations could be run, important substrate parameters needed to be entered in to the *Msub* block in the schematic. Microwave Impedance Calculator, *MWIJ 1.0* was used to calculate the width of the microstrip transmission line considering its characteristic impedance to be 50 Ω (See Figure 9). Following are the parameters used for Class A simulation by both programs:

Dielectric Thickness, D or H = 30 mil. Dielectric Constant, $\varepsilon_r = 3.38$.

Loss Tangent, tan(δ) = 0.0022. Thermal Conductivity = 0.64 W/m/°K.

Relative Permeability, Mur = 1. Conductivity = 5.8 E+7 for copper in PCB.

Foil Thickness, T = 1.4 mil, 1 oz Cu. Hu = 3.9 E+34 mil. Rough = 0 mil.

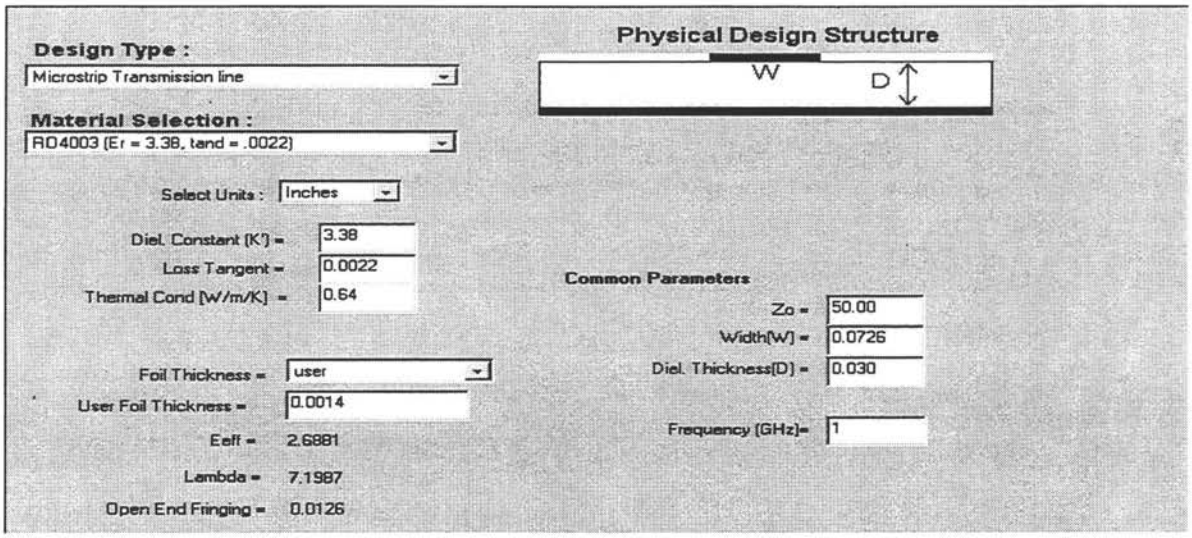

Fig 9. *MWIJ 1.0* Screenshot for Microstrip T Line (50 Ω) Width Calculation

Other parameters in the program were kept at default values. The width of the microstrip transmission line was found to be 72.6 mils.

Stability of RF Transistor

To obtain desired results from the amplifier, it needed to be unconditionally stable to prevent oscillation on a certain frequency range with the center at 1 GHz. There are a couple of ways to address the stability criteria of a 2-Port network i.e. our transistor (Refer to Chapter 3, Section 3 of [2]). The derivation of the stability criteria is based on S-Parameters. From a circuit designer's point of view, the necessary and sufficient condition for a transistor to be unconditionally stable can be described in terms of K and Δ factor. Sometimes, the K factor is identified as the Stern Stability Factor [4]. Following are the conditions :

$$K > 1 \quad and \quad |\Delta| < 1 \tag{17a}$$

Where $$K = \{1 - |S_{11}|^2 - |S_{22}|^2 + |\Delta|^2\}/\{2|S_{12}S_{21}|\} \tag{17b}$$

$$|\Delta| = S_{11}S_{22} - S_{12}S_{21} \tag{17c}$$

From a practical point of view, many microwave transistors available in the industry are potentially unstable with $K < 1$ and $|\Delta| < 1$. In the case of potentially unstable transistors, K values are such that $K < 1$ [2]. From the S-parameter file for the *mmbr901LT1* transistor available in the lab, it can be verified that the S-parameters for this transistor at 1 GHz are as follows :

$S_{11} = 0.2490 \angle -177.0547°$ $\qquad$ $S_{21} = 3.3784 \angle 68.9023°$

$S_{12} = 0.1289 \angle 72.4258°$ $\qquad$ $S_{22} = 0.4289 \angle -34.5020°$

Using equation (17b) and (17c), we find that $K = 0.9906$ and $\Delta = 0.3298 \angle -40.9709°$. As a result, our RF transistor exhibits a potentially unstable condition with $K = 0.9906 < 1$ and

$|\Delta| = 0.3298 < 1$. To stabilize the transistor, resistive loading was utilized by connecting a 9.1Ω resistor in series at the input port i.e. Port 1. Refer to Figure 10. R_s connected to Q1 is the stabilizing resistor. To verify that the RF transistor is indeed stable, HP-ADS simulation was run over a frequency range of 10 MHz to 6 GHz. The S-Parameters of the resistive loaded RF transistor, Q1 at 1 GHz were extracted from the simulation data file which are given below :

$S_{11} = 0.054 \angle 172.816°$ $S_{21} = 2.862 \angle 47.165°$

$S_{12} = 0.126 \angle 53.336°$ $S_{22} = 0.453 \angle -53.567°$

From above data, $K = 1.26 > 1$ & $|\Delta| = 0.3375 < 1$ were calculated using equation (17b) & (17c). Thus, the resistive loaded RF transistor in Figure 10 is unconditionally stable at 1 GHz.

Input & Output Matching Network

Using HP-ADS, simultaneous conjugate match SMZ1 & SMZ2 impedances of the resistive loaded RF transistor network were extracted. Simultaneous conjugate matching was used to design matching networks for both Port 1 and Port 2 for maximum power transfer from input to output i.e $SMZ1 = Z^*_{IN}$ and $SMZ2 = Z^*_{OUT}$ must be satisfied. For the matching purpose, the RF transistor Q1 with series resistor R_s is considered as the DUT or 2 – Port transistor network block. Using this block, an HP-ADS simulation is run in order to find out the new set of S-Parameters and SMZ1 & SMZ2 (Figure 10a). Figure 10 shows the stable 2-Port RF transistor network with input and output matching networks.

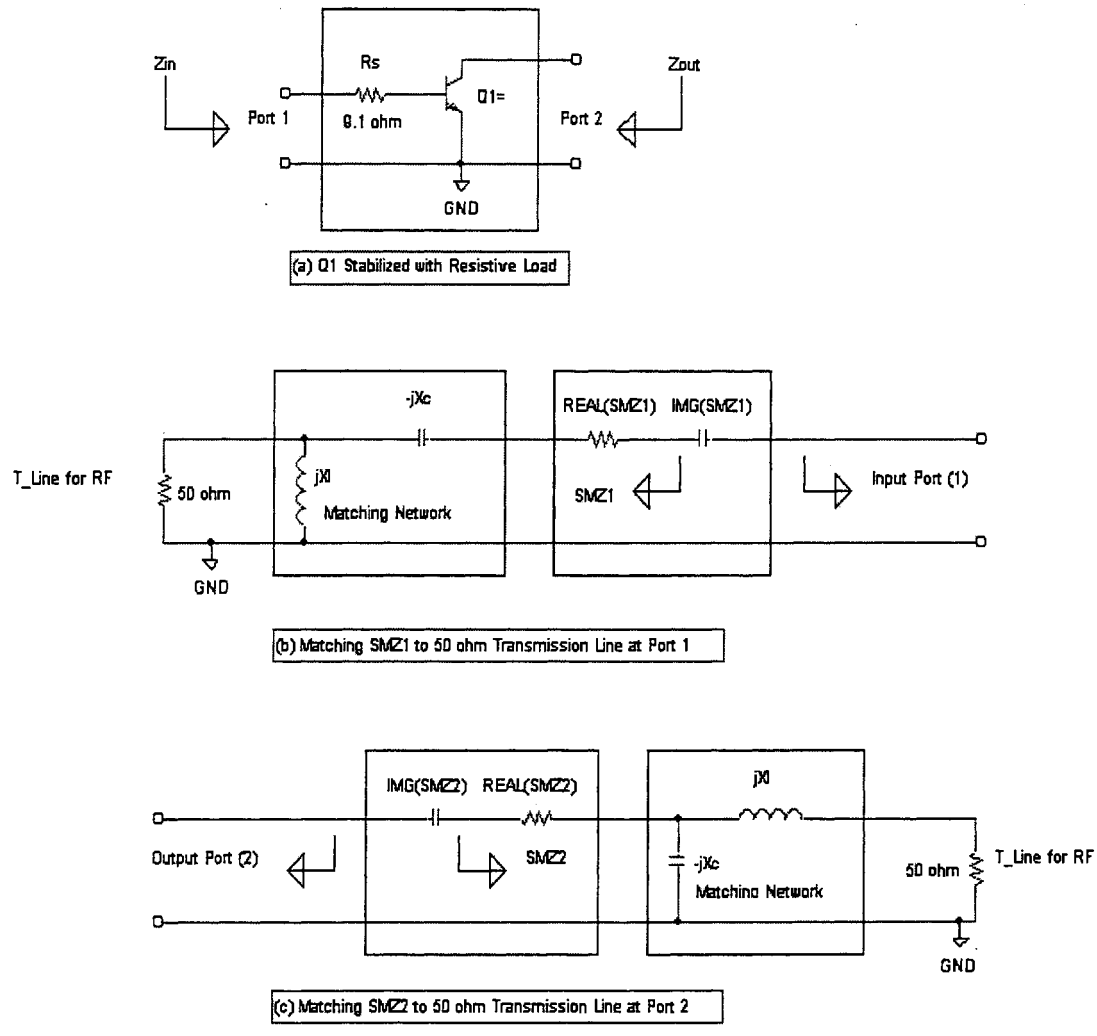

Fig 10. Stabilizes RF Transistor or DUT & Input-Output Matching Network

Simulation results yield the necessary values of SMZ1 and SMZ2 as follows :

$SMZ1 = R_{s1} - jX_{s1} = 25.836 - j7.225$ $\quad SMZ2 = 50.792 + j70.667$

$SMY1 = 0.0036 + j9.965E-3$ $\quad SMY2 = G_{s2} - jY_{s2} = 0.0064 - j8.932E-3$

L section matching networks were used to match the input and output impedances of the DUT to the 50 Ω transmission line [1] as described below. Refer to Figure (10b), adding

the matching network to the 50 Ω transmission line would yield an equivalent impedance (looking from Port 1 towards 50 Ω T_Line) of SMZ1.

$$\Rightarrow SMZ1 = [1/\{(1/R_p) + (1/j\omega L_1)\}] + [1/(j\omega C_1)] = R_{s1} - jX_{s1} \quad (18a)$$

After simplification and rearranging the real and imaginary parts on the right hand side of equation (18a), they can be equated to the resistance and reactance values of SMZ1 above.

$$\Rightarrow [R_p(\omega L_1)^2/\{(R_p)^2 + (\omega L_1)^2\}] = R_{s1} \quad (18b)$$

$$\& \Rightarrow [(1/\omega C_1) - \{(R_p)^2 \omega L_1\}/\{(R_p)^2 + (\omega L_1)^2\}] = X_{s1} \quad (18c)$$

Substituting, Quality Factor, $Q = [(\omega L)/R_p]$ (18d)

in equations (18a) and (18b), Q in terms of R_{s1} and $R_p \Rightarrow Q = [(R_{s1})/(R_p - R_{s1})]^{1/2}$ (18e)

As a result, Q = 1.034, L_1 = 8.232 nH, C_1 = 4.038 pF were obtained while R_p = 50 Ω.

According to Figure (10c), adding the matching network to the 50 Ω transmission line would yield an equivalent admittance (looking from Port 2 towards 50 Ω T_Line) of SMY2. For ease of calculation, admittance was used instead of impedance.

$$\Rightarrow SMY2 = [j\omega C_2 + \{1/(\omega L_2 + R_p)] = G_{s2} - jY_{s2} \quad (19a)$$

After simplification and rearranging the real and imaginary parts on the right hand side of equation (20a), they can be equated to the real and imaginary values of SMY2 above.

$$\Rightarrow G_{s2} = [(R_p)/\{(R_p)^2 + (\omega L_2)^2\}] + (j\omega C_2)] \quad (19b)$$

$$\& \Rightarrow Y_{s2} = [(\omega L_2)/\{(R_p)^2 + (\omega L_2)^2\} - \omega C_2] \quad (19c)$$

Using equation (19d), (20a) and (20b), Q in terms of G_{s2} and R_p as follows :

$$\Rightarrow Q = [(1 - R_p G_{s2})/(R_p G_{s2})]^{1/2} \quad (19d)$$

As a result, Q = 1.458, L_2 = 11.606 nH, C_2 = 0.064 pF were obtained while R_p = 50 Ω. After the matching network is connected, SMZ1 and SMZ2 will have new values satisfying the

simultaneous conjugate matching condition. A blocking capacitor (100 pF) was also connected at the output of the amplifier to prevent any DC signal from bias circuit leaking into the output port and disrupting useful measurement data.

Parasitics Consideration, PCB Layout & Circuit Tuning

Before the amplifier circuit can be assembled, a printed circuit board (PCB) needs to designed. For this purpose, parasitics elements need to be added to the resistors, capacitors and inductors used in the circuit. Since, at RF frequencies (1 GHz in this case), these circuit components will exhibit resistance, inductance and capacitance other than their lumped values which will change the overall amplifier performance. Besides, pads need to be added for creating circuit nodes on the PCB. To connect two or more circuit components to form a node, a *mlin* block (pad) was chosen from the HP-ADS menu. In order to ground the emitter of the RF transistor or any other circuit elements, a *mloc* block (pad) was used. Holes need to be drilled on these ground pad and tiny wires (this wire has an approximate inductance of 0.3 nH) are inserted through to the other side (the ground plane) of the PCB and soldered on both sides to create a practical circuit ground. A 0.3 nH inductor was connected between the *mloc* block and ground for every circuit element that is connected to the circuit ground on the PCB in the HP-ADS schematic environment. As a result, the simulation would produce results that are consistent with results obtained from actual PCB implemented amplifier circuit. After adding parasitics, the circuit elements needs to be tuned with the *tuner* in HP-ADS so that the resulting S-Parameters exhibit desired gain and simultaneous conjugate matching at 1 GHz. Figure 11 shows the models used for chip resistor, chip inductor and chip capacitor. Once the circuit has been tuned with parasitics taken into consideration, the layout of the PCB was done using *EAGLE Layout Editor 4.03*

for Windows. The RF portion of the amplifier circuit was built using surface mounted R, L, C's and a npn transistor (MMBR901LT1) available in the lab. The bias portion of the amplifier circuit was built using discrete R, L, C's and a pnp transistor (2N2907A) available in the lab.

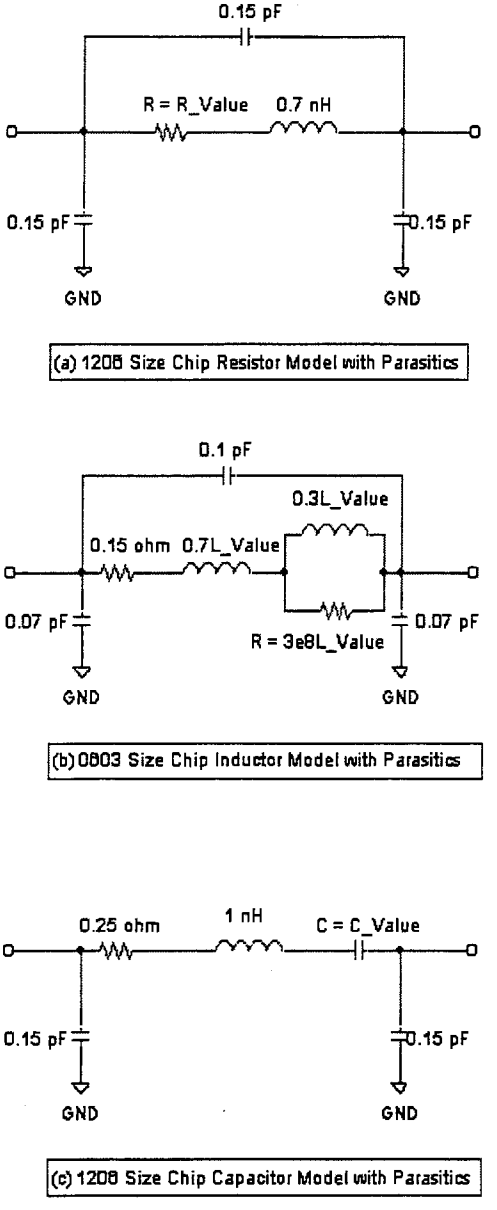

Fig 11. Amplifier Passive Circuit Component Models for Use at RF Frequency (1 GHz)

To connect the RF (npn) and bias (pnp) transistors and other passive elements (R, L, C) between the pads of particular width and length on the PCB, different amount of gaps were created during circuit layout. These important dimensions are given below :

Gap between pads for mounting Resistor = 90 mils.

Gap between pads for mounting Inductor = 30 mils.

Gap between pads for mounting Capacitor = 90 mils.

Gap between Base & Emitter pads of npn transistor = 75 mils.

Gap between Collector & Base or Emitter pads = 40 mils.

Gap between Base & Collector pads of pnp transistor = 350 mils.

Gap between Collector & Emitter pads of pnp transistor = 220 mils.

Gap between pads for mounting rectifying diode in the Bias circuit = 250 mils.

Gap between pads for mounting discrete Resistors in the Bias circuit = 250 mils.

Width of MLIN & MLOC pads = 100 mils.

Length of MLIN & MLOC pads = 200 mils.

After adding the pads and blocking capacitors and taking the parasitics into consideration, the circuit behavior (i.e. gain, matching, stability etc) will deviate from the initial design specifications. So, the circuit needs to be tuned to meet our design goal. In order to do this, each circuit component was tuned using the *Tuner* function in HP-ADS. First, the components on the input port and then the output port were tuned. After the tune up, the amplifier circuit produced better stability (K = 1.43) than before but gain (S_{21}) was fairly unchanged. The component values in some cases changed considerably from the theoretically found values described earlier.

The list of the R, L, C values for the RF portion of the amplifier circuit are given below:

Port #1 or Input Side	*Port #2 or Output Side*
$R_{Stability} = 9.1\ \Omega$	L2 = 11.317 nH ≈ 11 nH
L1 = 17.936 nH ≈ 18 nH	C2 = 1 pF
C1 = 3.435 pF ≈ 3.3 pF	C_block = 100 pF

A *Milling Machine* was used to fabricate the PCB for the amplifier circuit and then the circuit was assembled. The circuit was tested using a *HP 8573C* network analyzer in conjunction with HP 85047A S-Parameter test set. The stability curve for the tuned Class A amplifier which is *K vs Frequency* was obtained using HP-ADS is shown in Figure 12 below.

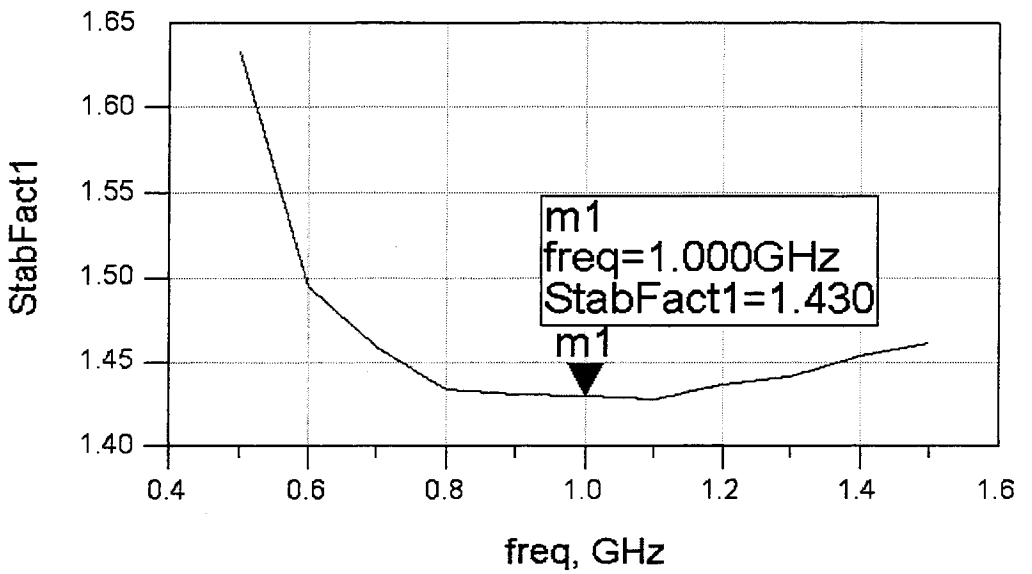

Fig 12. Stability Curve (K vs *f*) for Class A Amplifier

A comparison table for gain and S-Parameters for Class A amplifier obtained from network analyzer and HP-ADS simulation is given below :

Using HP-ADS Simulation				
Frequency	S_11 (dB)	S_21 (dB)	S_12 (dB)	S_22 (dB)
1 GHz	-19.58	9.2	-17.92	-10.9
Using HP Network Analyzer				
1 GHz	-34.77	9.02	-18.42	-15.13

The final Class A amplifier schematic from HP-ADS design environment is shown in Figure 13 below.

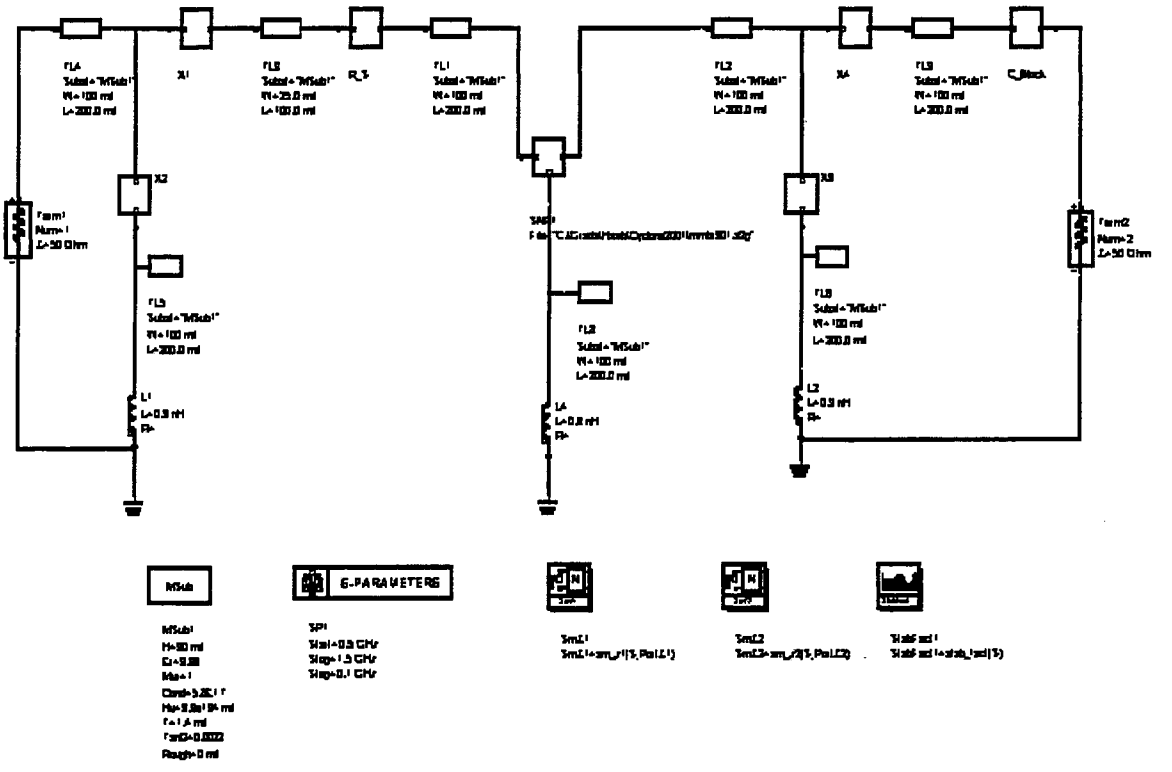

Fig 13. Final Schematic of Class A Amplifier from HP-ADS

Class C Design Process

In designing the Class C amplifier, the small signal S-parameters *for mmbr901LT1* could not be used. This is because a Class C amplifier operates in the nonlinear region and small signal parameters do not characterize the behavior of the RF transistor when used to design amplifiers for power application. A set of large signal S-parameters is needed to characterize the transistor. But measurement of large signal S-parameters is complicated and not perfectly defined [2]. Due to this constraint, HP-ADS simulation tool could not be used with a S-parameter device to aid the Class C amplifier design process. Figure 14 illustrates a Class C amplifier.

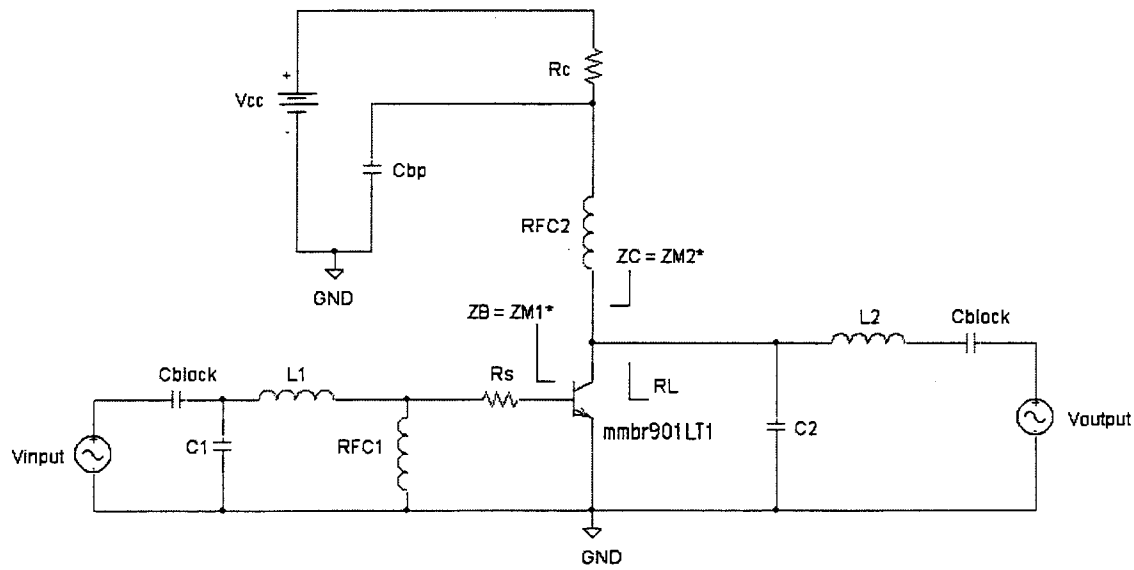

Fig 14. Class C Amplifier (Mix-Mode) with Manual Bias

The emitter is grounded and the input RFC1 = 68 nH was used to set the operating point value of the base to emitter voltage to zero. For an input RF signal, the RFC acts as an open circuit so this signal can turn on the transistor and make it conduct. The output matching network needs to have a high Q value in order to suppress the higher order harmonics and pass the fundamental amplified signal. The BJT based Class C amplifiers are generally called Class C mixed-mode amplifiers [4]. Rather than true Class C operation where there is a parallel tuned LC circuit at the output, Class C mixed mode is used in PAs using a BJT. This is due to difficulty in providing bias and drive for true Class C operation [4]. Its operation can be predicted through numerical analysis or by using transistor manufacturer supplied *large signal impedances* [4]. Large signal impedances (Impedances looking into the BJT collector, Z_C & base, Z_B) are valid only at frequencies and power levels they are measured at [4]. Since these resources were not available for the *mmbr901LT1* transistor, an alternative approach using the concept of output load was used to design the Class C amplifier [11]. The calculations for this method are given below :

Operating Point, $I_C = 20$ mA & $V_{CE} = 10$ V.

Minimum Collector Current, $I_{C\text{-}min} = 0$.

Collector Voltage at Saturation, $V_{CE\text{-}Sat} = 3$ V (Chosen by trial and error because Load Line Slope = $1/R_L$ and making the slope high enough would ensure the conduction angle much less than 180° and thus Class C operation possible)

Output Load, $R_L = (10 - 3)/(0.020) = 350\ \Omega$

The RF transistor was stabilized with a 9.1 Ω resistor in the same way as was done for Class A amplifier using HP-ADS. Using *HP 8753C* network analyzer, the input impedance was

measured as $Z_{IN} = Z_{M1}^* = 33.37 + j\ 22.98\ \Omega$. Using the conjugate matching concept, Z_{IN} and R_L were matched to 50 Ω transmission line as was done earlier for Class A amplifier. 100 pF blocking capacitors were connected both at input and output as shown in Figure 14 for protecting test instruments from DC signal leakage.

The matching network circuit element values are given below :

Port #1 or Input Side	*Port #2 or Output Side*
$R_{Stability} = 9.1\ \Omega$	L2 = 21.06 nH ≈ 21 nH
L1 = 3.75 nH ≈ 3.9 nH	C2 = 1.053 pF ≈ 1 pF
C1 = 2.26 pF ≈ 2.2 pF	C_block = 100 pF

Another RF choke RFC2 = 110 nH is connected between the RF transistor collector and bias circuit. R_C and C_{BP} were kept at the same value as was used in Class A design. The PCB for the Class C amplifier was designed and pads were added with necessary air gaps to solder circuit elements using the same procedures as was used for Class A amplifier.

CHAPTER 5. TEST SETUP & EXPERIMENTATION

After the amplifier circuit was designed, a test bench was set up to apply signal to the input of the amplifier under test and measure the necessary output powers since the method of AM-AM and AM-PM measurements in this experiment were done using only power measurements. A FLUKE 6060B RF signal generator was used to provide an input signal that contained both amplitude and phase modulation. The carrier frequency in this generator was set to 1 GHz ($\omega = 2\pi E{+}9$ *rad/s*). In this signal generator, different power levels, AM and FM modulations can be applied using pertinent control buttons and menus. Details on how to use it can be found in the operating manual. An HP 3310A function generator was used to provide the baseband or modulating signal. Since the RF signal bandwidth $2\Delta\omega$ is centered around ω and $\omega >> \Delta\omega$, a 20 kHz sine wave was used as the baseband signal. The HIGH input signal from the function generator was connected to the MOD_INPUT of the RF signal generator with its EXT_AM and EXT_FM turned on. The AM and FM modulation index were set at 50 % and 6 kHz/dev respectively. Other values could be used as long as it did not affect the bias point stability. It should be noted that increasing or decreasing the AM index with input power level between 10 dBm and 20 dBm would change the bias current of the NDUT from its desired value of 20 mA considerably. The OUTPUT LEVEL control in the function generator was adjusted so that optimum modulation (neither high or low i.e. baseband sinewave with 1 V peak) of the carrier signal can be sustained. The RF signal generator became uncalibrated when the power level was set to 10 dBm and the data displayed on the generator then does not actually represent the power available at its

RF_OUTPUT. Since, testing needs to be done for power levels from 0 to 20 dBm, a Mini-Circuit's pre-amplifier ZFL-1000VH2 was used. By using the pre-amplifier, power levels set far below 10 dBm at the RF generator can be amplified to the range between 10 to 20 dBm and thus applied as the actual input signal to the Class A or C amplifier. Since, there would not be any need to set the power level at the RF generator in the range between 10 to 20 dBm, the RF generator then does not become uncalibrated. It was then necessary to measure the power available at the output of the pre-amplifier by utilizing a HP 436A power meter. The power meter was also used to measure the power (carrier component) available at the output of the NDUT. Specifications for the pre-amplifier can be found at http://www.mini-circuits.com. An HP3478A multimeter, HP 6205B dual dc power supply and HP 6237B triple output power supply were used to provide necessary dc power to the amplifier and preamplifier circuit used in the experimentation and also to monitor proper bias condition. After connecting the output of the preamplifier to the input of the NDUT, its output port was connected to the RF_INPUT of the HP 8569A spectrum analyzer. The spectrum analyzer frequency was set to 1 GHz since that is our center frequency. The vertical calibration was set to 10 dB/div with the reference power level of the analyzer at 30 dBm. The amount of signal attenuation was chosen to be 40 dB while the horizontal calibration or span was set at 20 kHz/div. The rest of the control settings were kept at default values since their variations did not affect the measurements. These control settings were chosen to clearly display the carrier, lower and upper sideband components of the output spectrum available at the output port of the NDUT. This was essential since both the input and output power levels of the lower and upper sidebands had to be measured from the grid display of the spectrum analyzer. Besides, these data need to be as precise as possible. Measurements of the lower

and upper sideband power levels were taken a couple of times to make sure the variations in the measurements are minimal since ambient temperature, bias condition and temperature of the pre-amplifier changes over time and these factors do affect the test condition. A complete block diagram of the test setup with necessary identification of the control knobs for different instruments is shown in Figure 15.

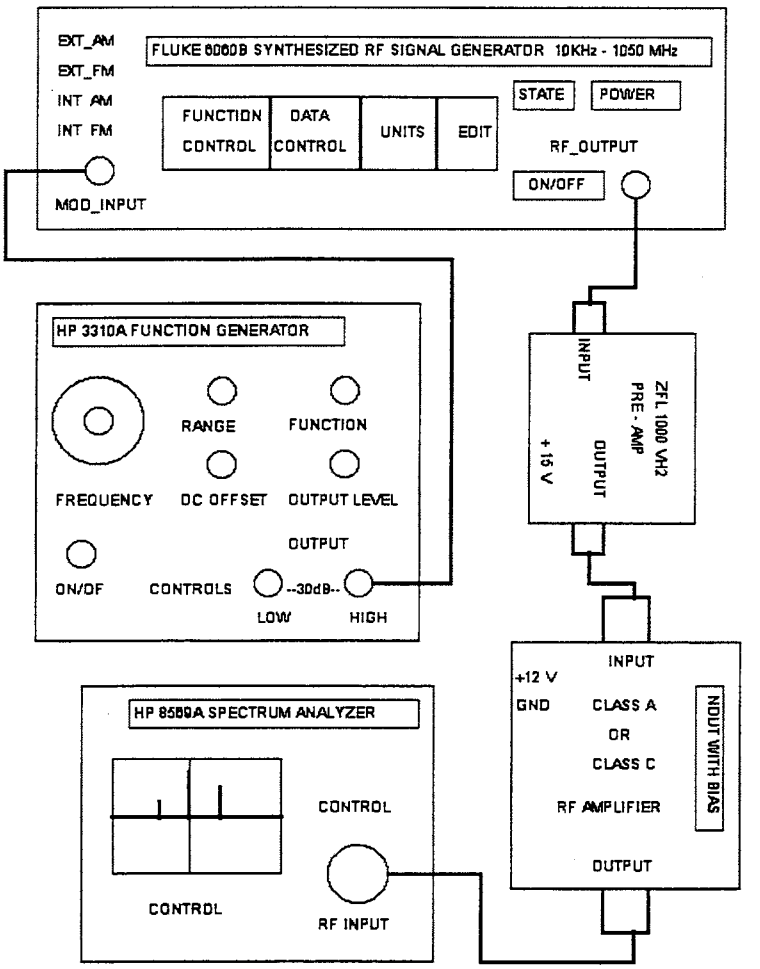

Fig 15. Test Setup for AM-AM and AM-PM Measurements of RF Power Amplifier

Some of the instruments are not drawn exactly. Details about the control panel of any instruments and their settings used in this experiment can be obtained from the user manuals. When the input signal is applied and the NDUT is properly biased with necessary instrument settings in place, the spectrum analyzer would display three unequal spectral components or tones of the output signal. According to Figure 14, the spectral component at the center represents the carrier power level at 1 GHz. The right and the left components represent the upper sideband and lower sideband power level. First, the output from the RF signal generator which is the actual input signal to the amplifier circuit is applied to the input of the spectrum analyzer in order to measure the power levels of the carrier, upper sideband and lower sideband at different input levels. Then the output of the amplifier circuit was applied to the input of the spectrum generator so that output power levels for carrier, upper sideband and lower sideband can be measured. These data for different power levels are utilized by equations discussed in the ANALYTIC APPROACH section of this thesis report to obtain important parameter values and measurements. For the Class A power amplifier measurements, the AM and FM index were kept constant i.e. 50% and 6 kHz/dev respectively. This is due to the fact that bias point remains stable for all input power levels applied from the RF signal generator for the Class A amplifier. In the case of Class C power amplifier, the bias current will change as different input power is applied at the amplifier input. Since the Class C amplifier is biased in the cutoff region, the base of the RF transistor in the amplifier has a negative bias. So, the drive signal is the RF sinewave with different power levels applied one at a time to the input. The positive cycle of this signal is responsible for turning the RF transistor on for a period of time when collector current flows. Different input power level would produce a different collector current. The experiment

focuses on comparing the AM to AM and AM to PM performance of a Class A and Class C power amplifier when I_C = 20 mA and V_{CE} = 10 V at different power level. Due to reverse bias in the emitter-base junction of the RF transistor, the portion of the input RF signal from the RF generator overcomes the negative bias to cause the collector current to flow. Experiments were performed with different input power levels to see at what particular input power the Class C amplifier has a collector current equal to 20 mA. For different trials of this experiment, this input power level tends to vary by 1 to 3 dBm. On one instance, the collector current reached 20 mA for an input power of 10.5 dBm while on another trial 12 dBm input power resulted in the same collector current. Unlike the Class A testing procedure where the bias point was maintained by the bias controller circuit, here we need to tweak the RF generator power level so that the amplifier collector current is 20 mA. Once this power level is set, the input power level was increased in increments of one dBm and necessary power measurements were recorded from the spectrum analyzer display. It needs to be mentioned that in the spectrum analyzer, the center frequency dial was set between 998 and 999 MHz, so that the carrier, upper and lower sideband spectral components can be displayed properly. Providing too much power from the RF generator would increase the collector current beyond 20 mA which would still give us AM-AM and AM-PM conversion. However the collector current should not exceed 30 mA since that is the maximum current the *mmbr901LT1* is designed for. The Class C amplifier designed is very sensitive to the input RF power RF power level. When the collector current increased beyond 20 mA, the AM index in the RF generator was decreased to stabilize it to its previous value. The opposite was done when the collector current decreased below 20 mA. Besides, great care should be taken while increasing the input RF power level so that the collector current does

not increase to a higher value abruptly. Not doing so on some occasions caused the RF transistor to burn out. A new RF transistor was soldered on the PCB which would change the circuit characteristics from the previous one. After tuning the new circuit and the test instruments settings, testing could be started as described earlier.

CHAPTER 6. RESULTS AND DISCUSSION

The unequal three-tone test signal method is used to conduct experiments on a Class A and Class C microwave power amplifier in order to measure the AM-AM and AM-PM distortion factor at specific input power level. The whole experiment is based on the short technical paper by F. M. Ghannouchi, H. Wakana and M. Tanaka [8]. According to the paper, the experiment investigates the AM-AM and AM-PM distortions of a high power and high gain traveling wave tube (TWT) amplifier using power measurements. In this thesis, efforts are made to prove that this same technique can be used to measure the AM-AM and AM-PM conversion factors of solid state microwave amplifiers such as Class A and Class C power amplifier based on *mmbr901LT1* microwave transistor. In a Class A amplifier, a high degree of linearity was observed when very low input signals were applied. As a result, it was extremely hard to measure the AM-AM and AM-PM conversion coefficients using the test setup described earlier. When the amplifier was operating well inside its linear region, the AM-AM compression factor would be zero since theoretically $\{\Delta V_{out}/V_{out}\}/\{\Delta V_{in}/V_{in}\}$ would be equal to 1. When very low level signals i.e. power levels below 1-dB compression point, were applied, no compression was present. Since all power measurements were recorded from the spectrum analyzer display and resolution of the vertical grid was not precise for low level measurements, some inaccuracies in the recorded data yielded negative compression value for input power levels between –21 dBm to –12 dBm. For these input levels, compression would actually be set to zero for the purpose of other calculations and plot generation. Similarly, the AM-PM conversion factor calculation was also affected due

to these inherent problem in the data. But most power measurement data at higher input power level yielded satisfactory results. When both the Class A and Class C amplifiers were driven far into the saturation or nonlinear region (Class C is always nonlinear), changes in the phase of RF voltage at the amplifier output were clearly evident due to amplitude modulation in the voltage at the amplifier input. For the Class A amplifier AM-PM conversion started at the input level of –12.32 dBm. Due to the mathematical nature of the closed form expression for calculating AM-PM conversion factor, low level input power resulted in error. This was the case for input power level less than –13 dBm where other parameters (c, x_1, R_1) used to calculate K_p produced a square root of a negative number which cannot be possible [8]. It should be mentioned again that the input signal must contain both amplitude and phase modulation in order to generate three unequal tones. Due to the PM sidebands being out phase by 90° from each other, the composite left hand side band (both AM & PM components of the input signal added) will be lower in amplitude than the right hand composite side band. The difference between the upper and lower side bands were kept at 10 to 12 dB for most values of the input signal. But this difference decreased to as low as 4 dB at higher input power level. During the experiment, one important observation about the difference between USB and LSB was made. When the AM index was increased, the difference increased. On the other hand, increasing the EXT_FM in the RF signal generator or the FM index reduced the difference. Reducing the AM index below 50% increased the power in the carrier component of the output signal. For low level inputs, the value of R_2 is small as compared to R_1. As a result, the intersection points of the two circles were not well defined as it is obvious from the graphical solution of the UTTS method. For details aboutthe graphical solution, refer to the IEEE short paper by F. M. Ghannouchi, H. Wakana,

and M. Tanaka [8]. As the input power was varied, the gain of the amplifier calculated from the recorded data changed. It was evident from the analytic approach that the change in the operating gain affected the carrier and sidebands proportionately. So, the c and K_p at various input levels will not change due to gain variations. This was proved when this same experiment was run several times under different testing conditions where the amplifier gain changed by a 1 to 2 dB.

Nonlinear Distortion Characterization Plot for Class A Amplifier

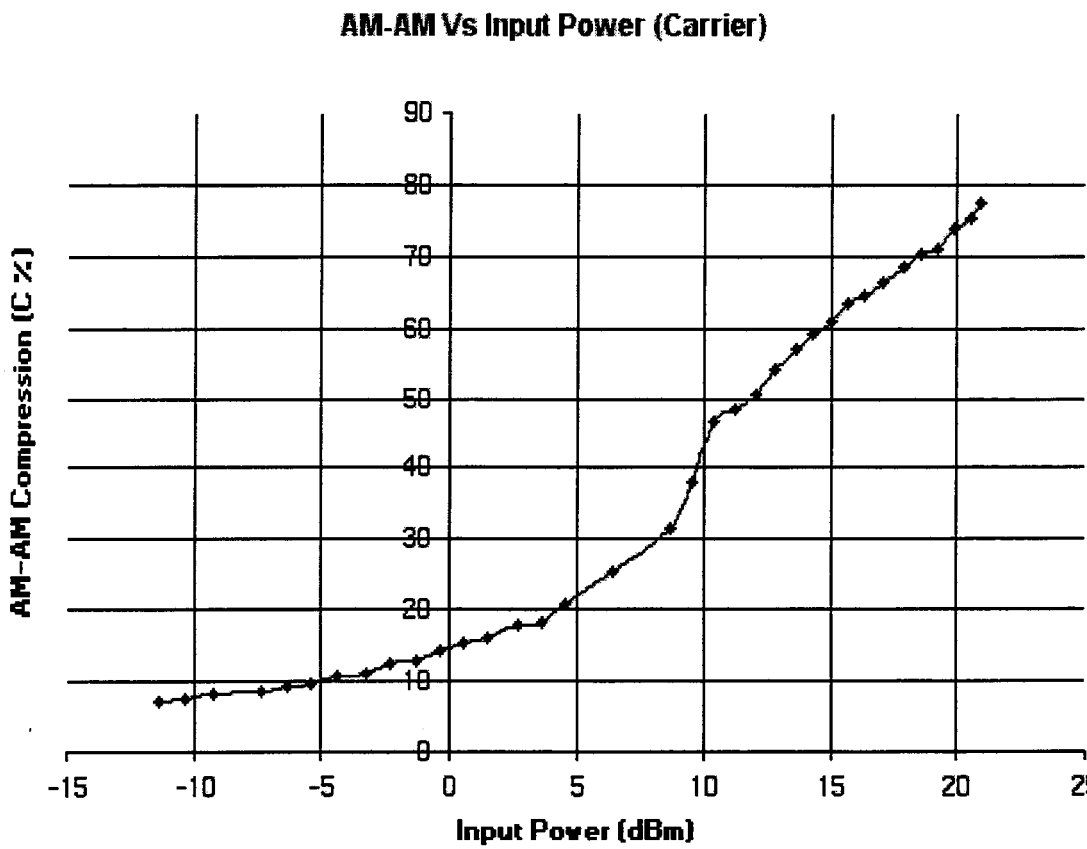

Fig 16. AM-AM Compression Curve

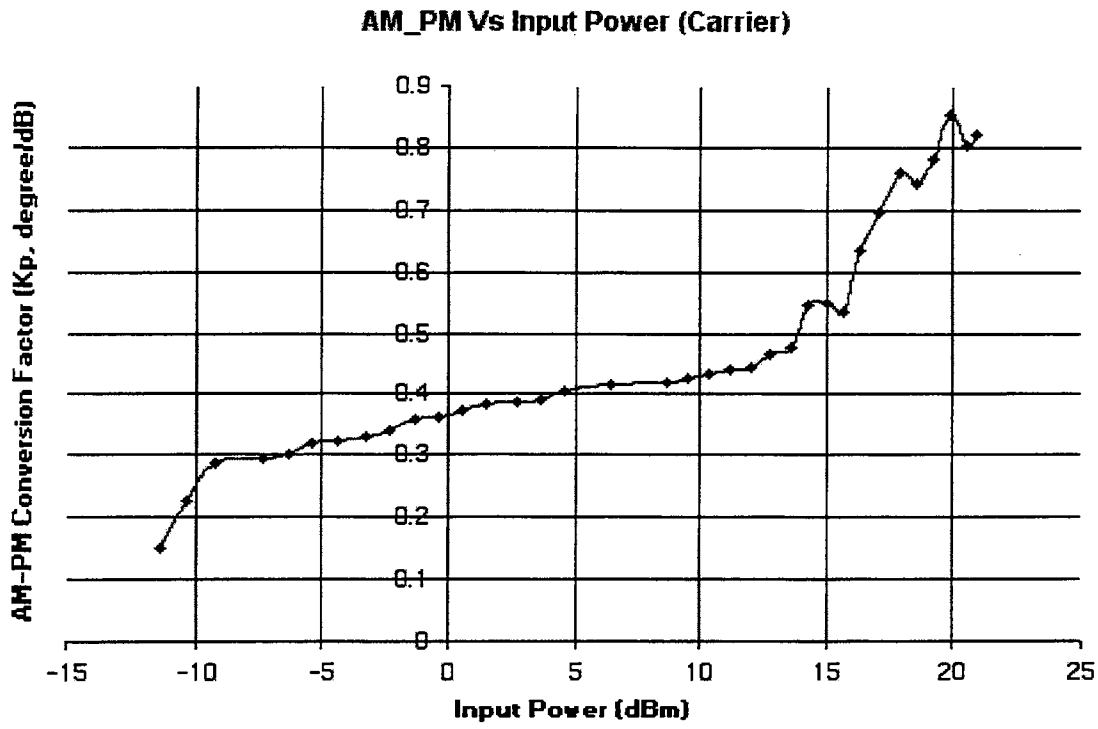

Fig 17. AM-PM Conversion Coefficient Curve

According to Figure 16, the AM-AM compression is zero below –12.32 dBm. As the amplifier is driven more and more towards nonlinear region, compression of the input signal (AM portion) envelope becomes obvious. When the amplifier is completely saturated, the compression of the AM envelope approaches close to 0.9 or 90 % though theoretically it should have been 1 or100 %. If it was possible to increase the input power level beyond 21 dBm, the compression factor might have reached 100 %. Since the amplifier was designed to generate a maximum power of 100 mW, increasing the input too much beyond 21 dBm would have damaged it. At input power levels below -3 dBm, the increase in compression

was not very high. Due to AM modulation in the input, phase modulation is generated in the output signal. According to Figure 17, the AM-PM increases with higher input power. Since the Class A amplifier (small-signal amplifier) has a high degree of linearity, the AM-PM conversion coefficient typically remains less than one [10]. For low level input power i.e. below -5 dBm, some irregularities in the K_p value is evident.

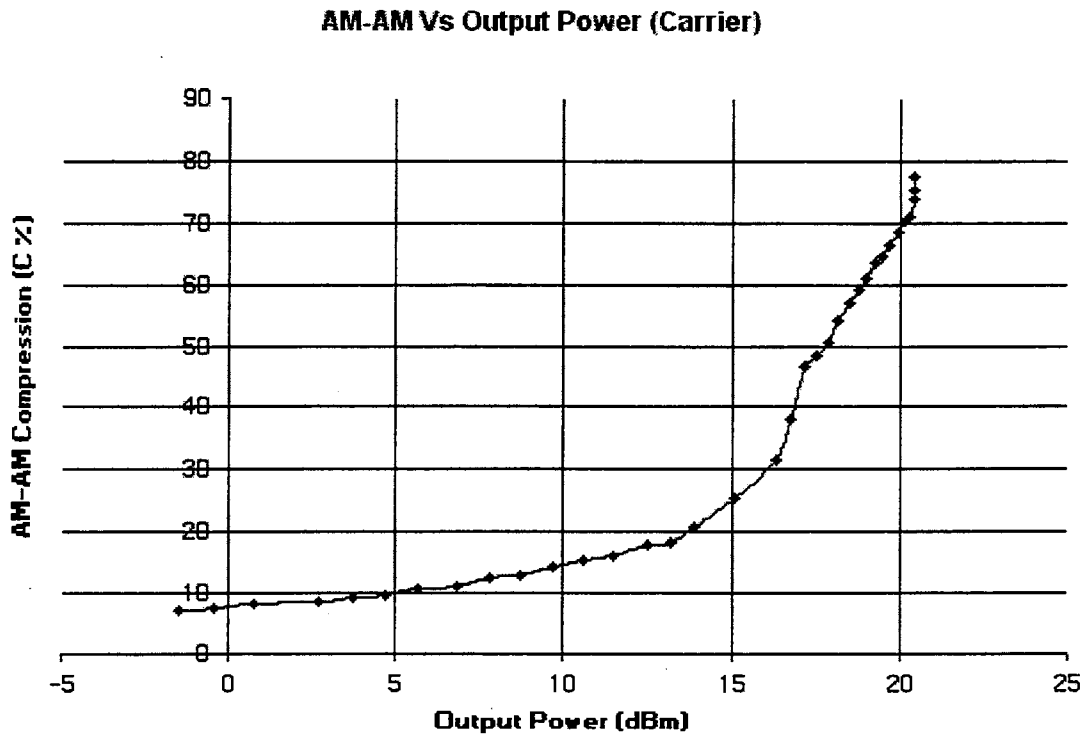

Fig 18. AM-AM Compression Curve

In the above figure, the compression curve is similar to Figure 16 but shifted to the right. When the output power is above 14 dBm, the AM envelope of the input signal experiences considerable compression but the compression value becomes undefined above 20 dBm.

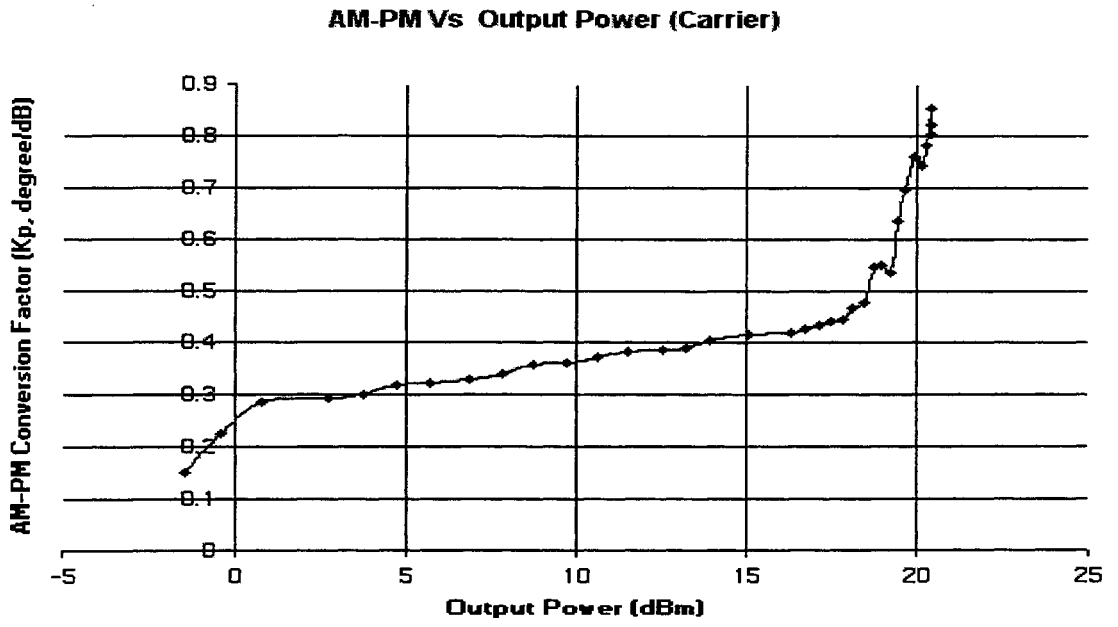

Fig 19. AM-PM Conversion Curve

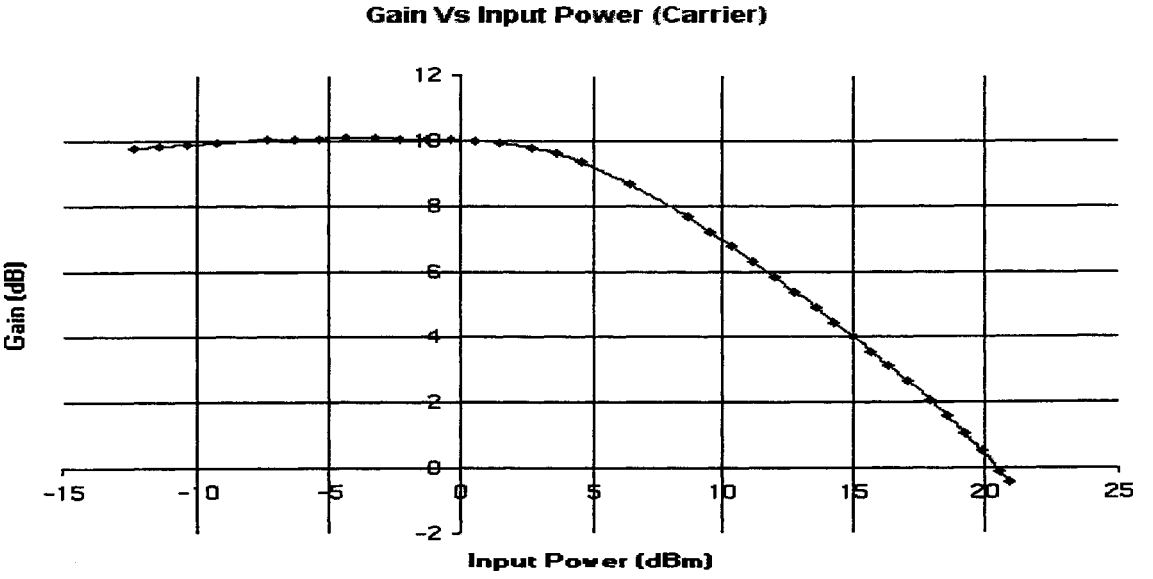

Fig 20. Gain Variation with Input Power

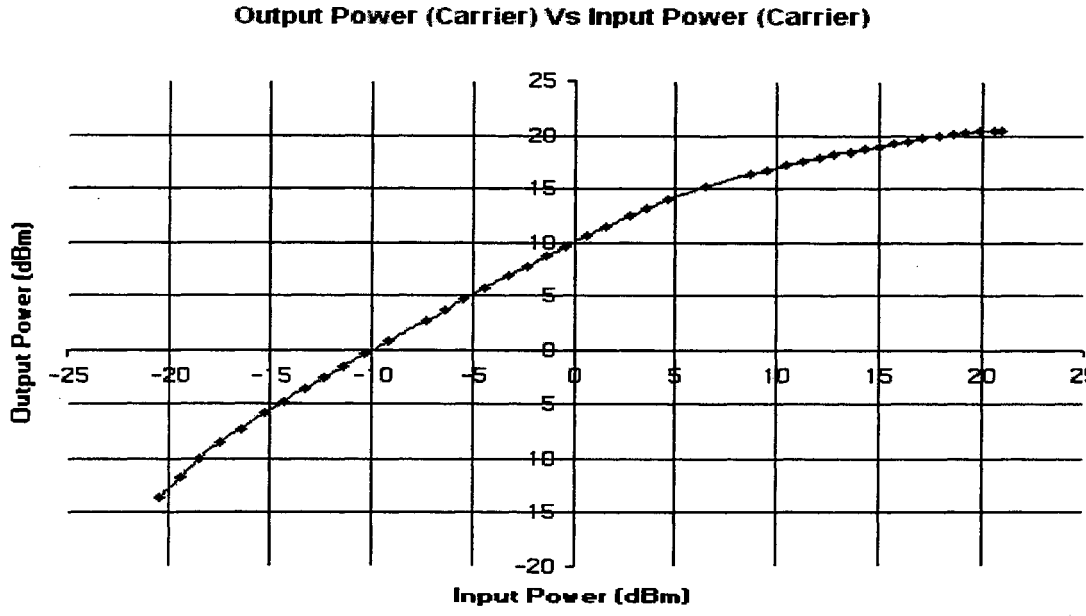

Fig 21. Output Power as a Function of Input

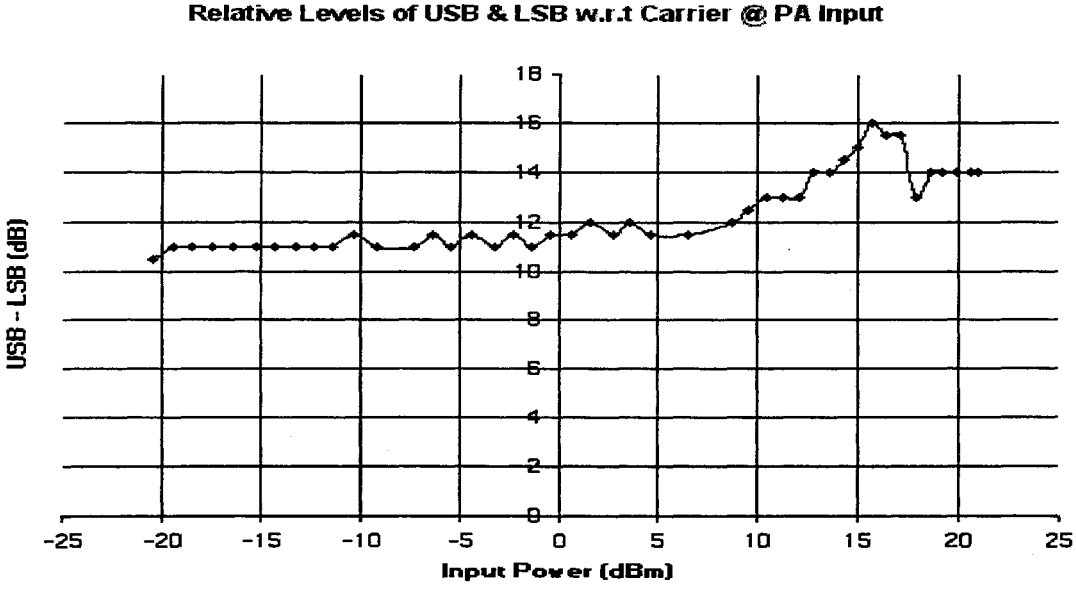

Fig 22. Variation in Relative Levels of Input Signal Sidebands with Input Power

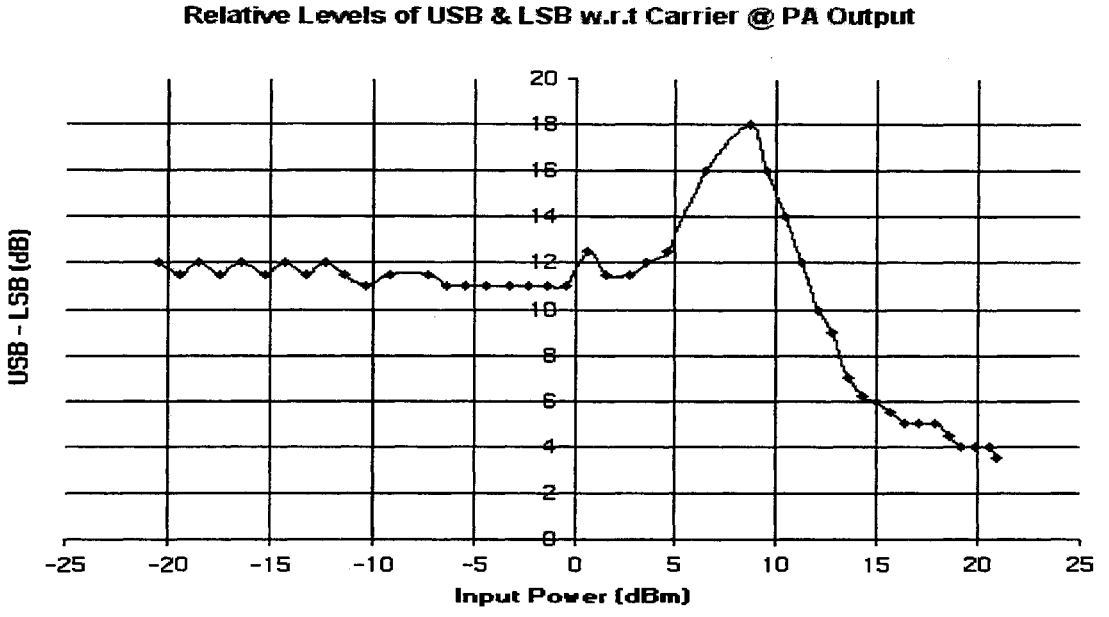

Fig 23. Variation in Relative Levels of Output Signal Sidebands with Input Power

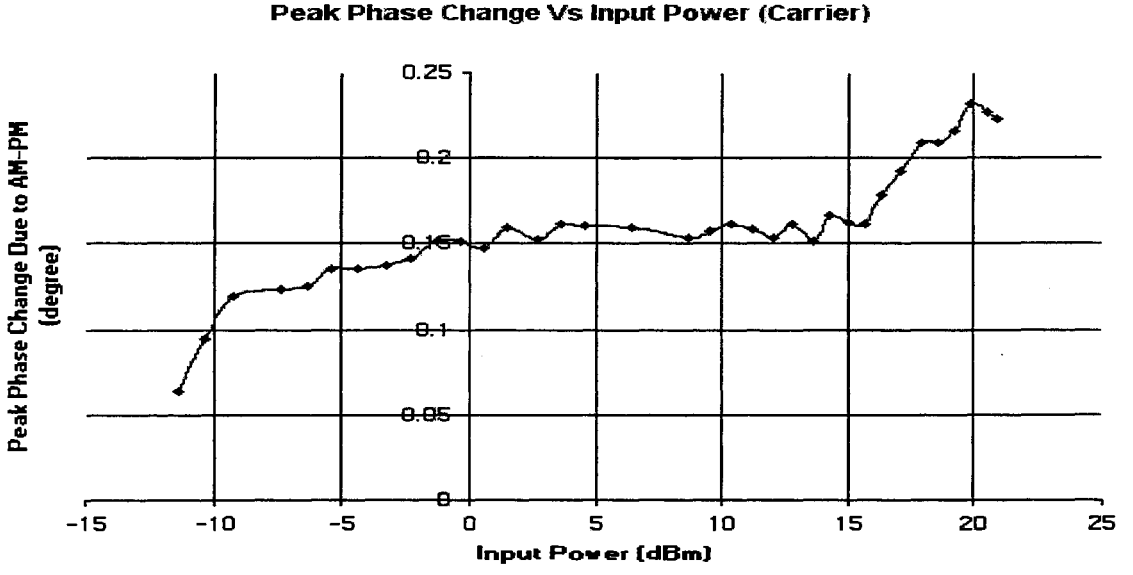

Fig 24. Peak Phase Variation at Output of DUT with Input Power

Figure 22 shows the relative levels of the upper and lower sideband components of the input signal as input signal power is varied. The difference between the right-hand and left-hand side bands remained between 11-11.5 dB for the linear region of operation but this difference begins to increase in the nonlinear region (beyond 5 dBm) and starts to decrease when the PA is driven far into the saturation region. At the output of the PA, when measurements were taken, the difference between the upper and lower sidebands was much different than that of the input. This is due to the extra AM and extra PM generated in the PA. According to Figure 23, the difference between the upper and lower sidebands at the PA output remained between 11-12.5 dB for the linear region but increases to 18 dB when input power is at 9 dBm (nonlinear region). This difference decreases when the PA is driven far into the saturation region. In this region (beyond 10 dBm), the difference varies between 15 – 4 dB. While at the input, the variation in this difference was limited to 16 – 13 dB (Refer to Figure 22 beyond 10 dBm input power). When the amplifier is operating in its nonlinear region, AM-PM conversion results in the peak phase change ($\Delta\theta$) of the input signal as shown in Figure 24. When input power is increased beyond 15 dBm, positive phase change occurs in an increasing manner. Though at some higher power levels, the peak phase change decreased, overall the curve in Figure 24 has a positive slope. The reason for this kind of behavior is due to error in measurement process since precise data read out from the spectrum analyzer display was difficult for smaller variations at the PA output. Similar explanations can be drawn from the plots generated for Class C amplifier data which are provided in the subsequent pages of this section.

Nonlinear Distortion Characterization Plot for Class C Amplifier

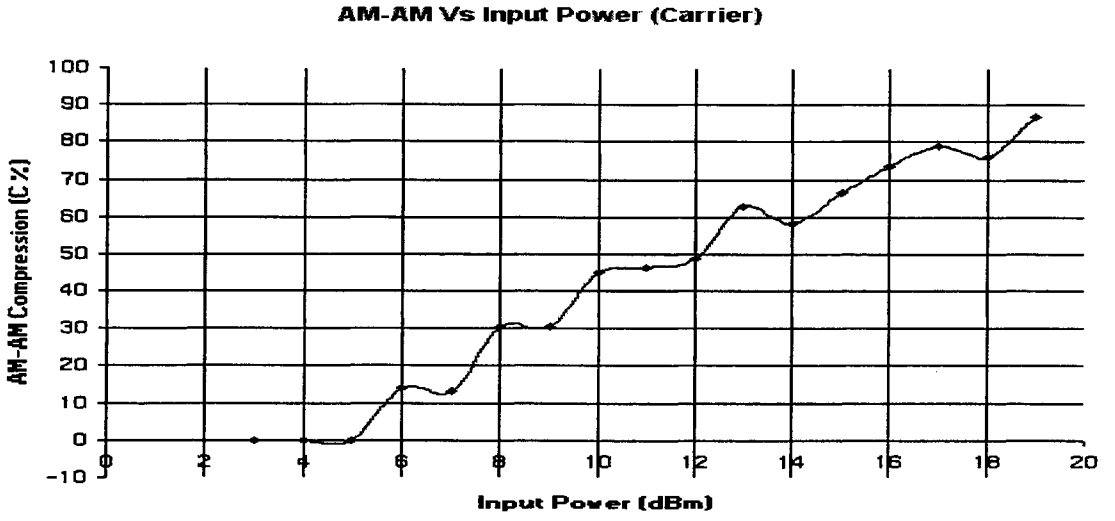

Fig 25. AM-AM Compression Curve

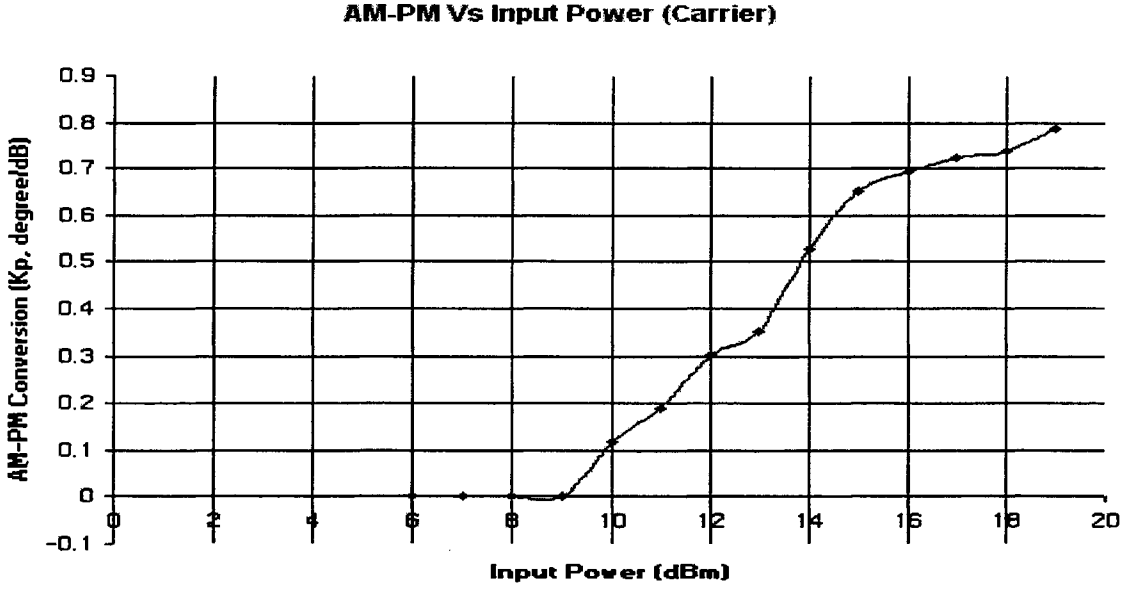

Fig 26. AM-PM Conversion Coefficient Curve

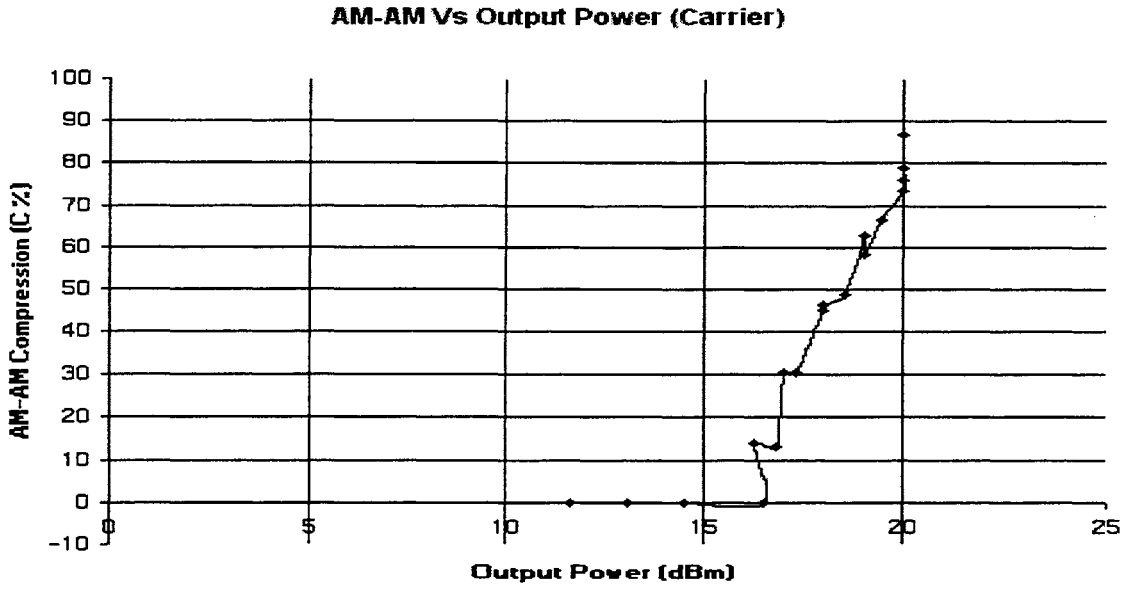

Fig 27. AM-AM Compression Curve

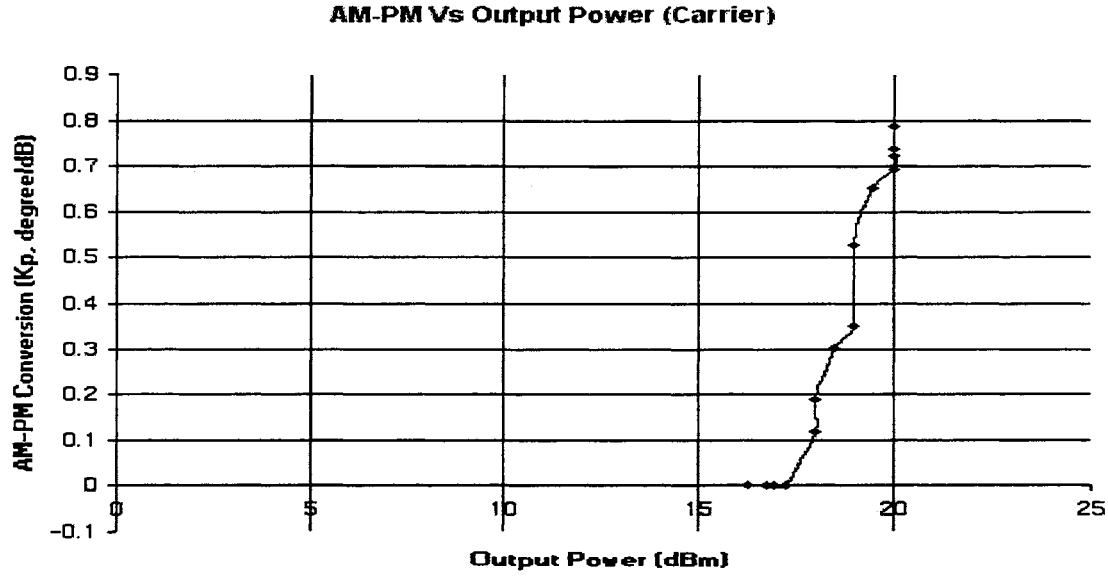

Fig 28. AM-PM Conversion Coefficient Curve

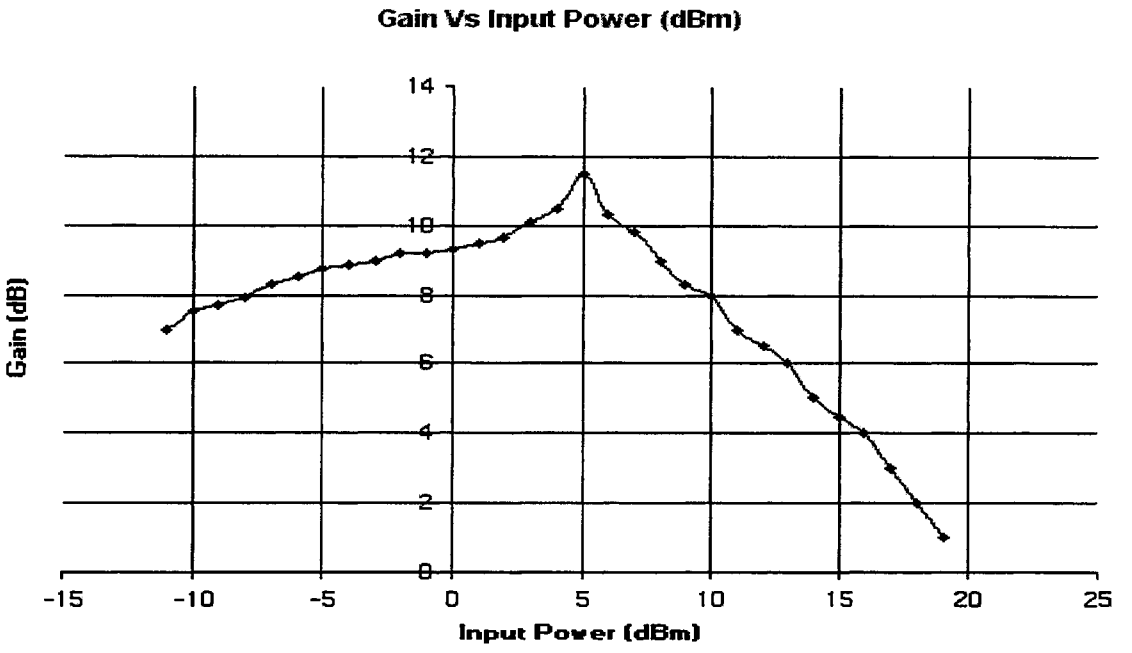

Fig 29. Gain Variation with Input Power

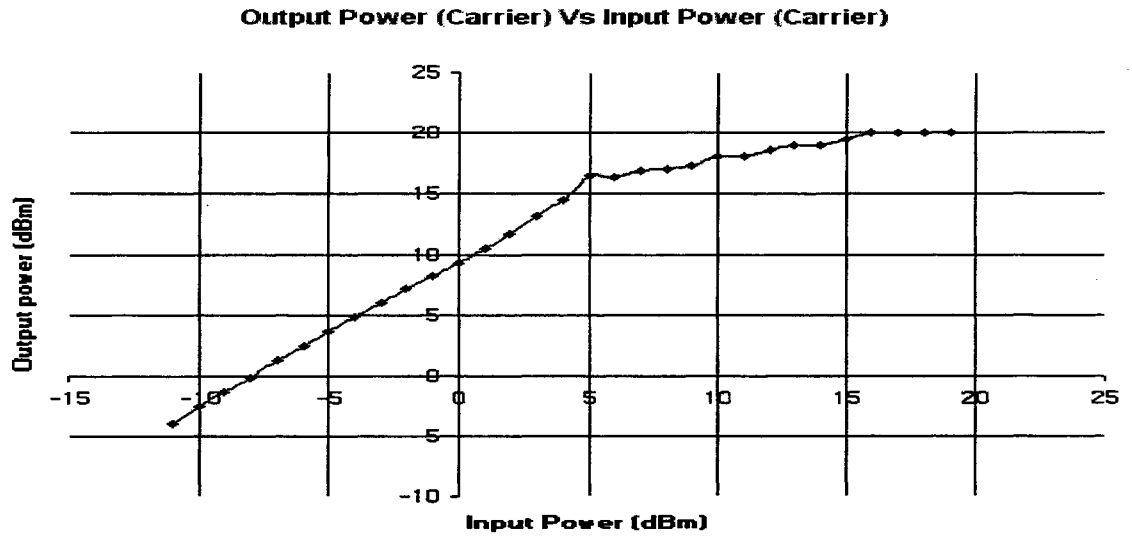

Fig 30. Output Power as a Function of Input

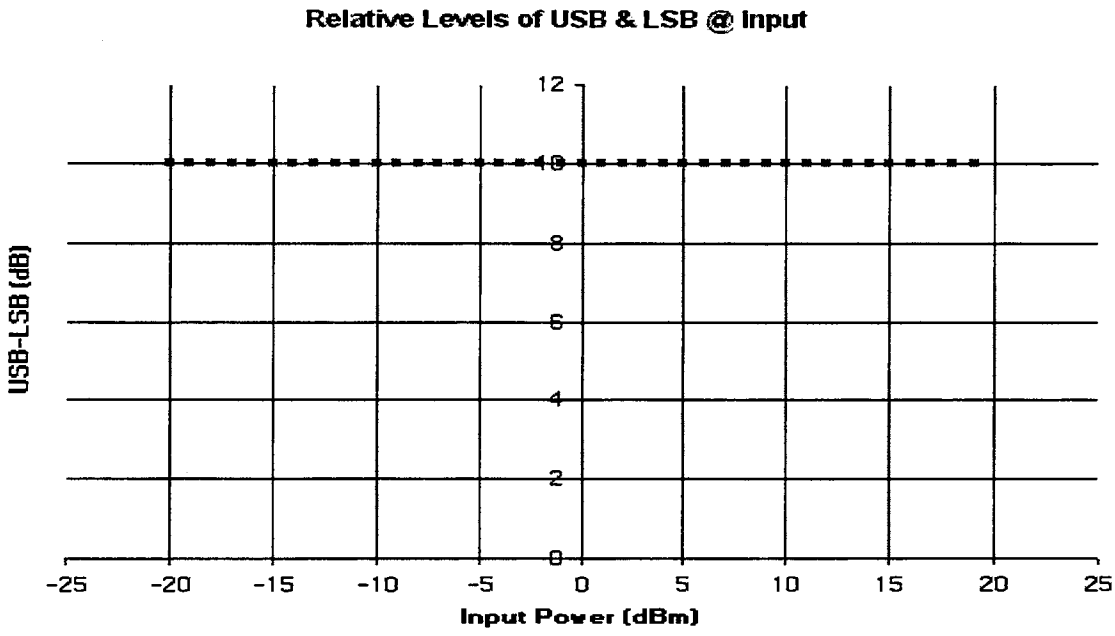

Fig 31. Variation in Relative Levels of Input Signal Sidebands with Input Power

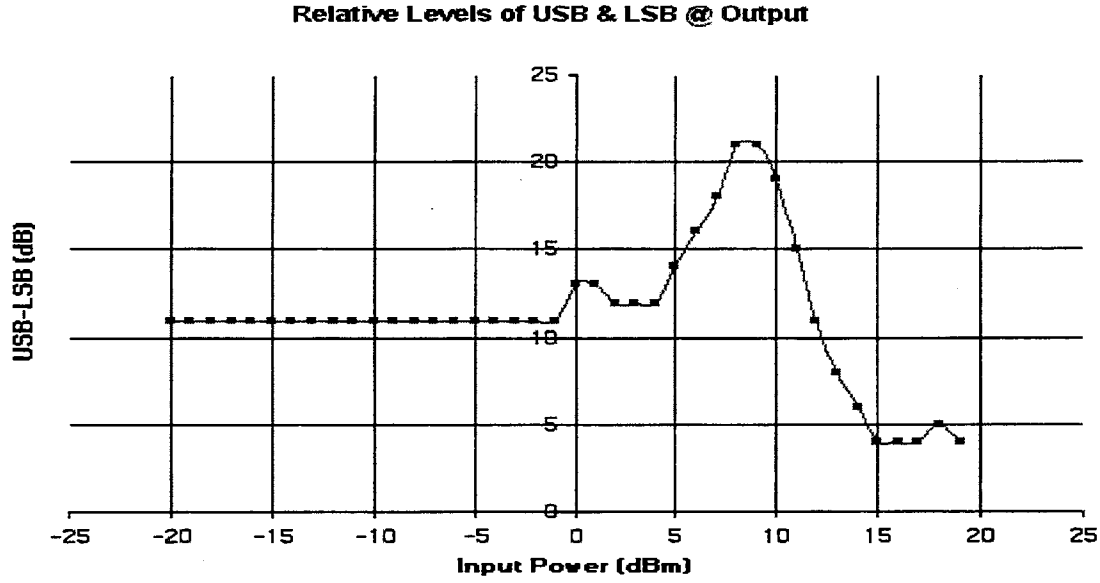

Fig 32. Variation in Relative Levels of Output Signal Sidebands with Input Power

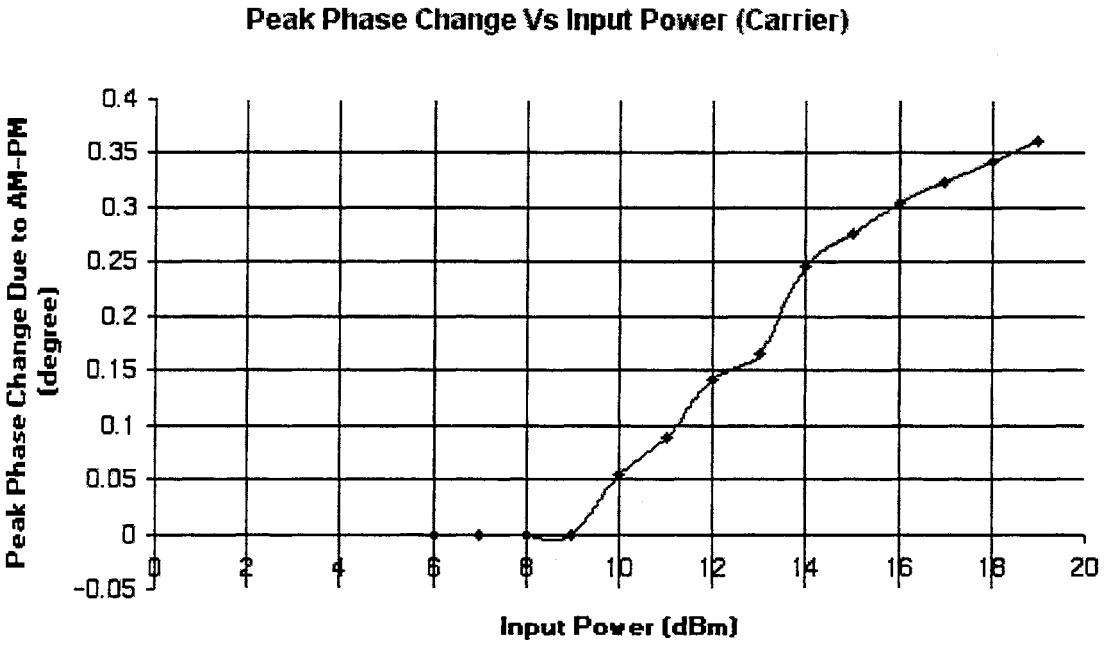

Fig 33. Peak Phase Variation at Output of DUT with Input Power

CHAPTER 7. CONCLUSIONS

In this thesis project, the main goal was to investigate a new technique (UTTS) for measuring AM to AM compression and AM to PM conversion coefficients of Class A and Class C solid-state power amplifiers. The design specifications (i.e. input-output, gain characteristics, operating frequency etc) of the solid state amplifiers used in the experimentation can be chosen by the designer in conjunction with the technical specifications provided by the manufacturers of the microwave transistor (*mmbr901LT1*). The details of the design process and important design parameters of the NDUTs used were discussed earlier in the *PA Design Considerations* part of this report. The Unequal Three Tone Technique or the UTTS method has already proven successful for measuring AM-AM and AM-PM distortion factors of a high power traveling wave tube amplifier (TWTA). The experimentation technique was based on power measurements as described in the short paper by *F.M Ghannouchi, H. Wakana and M. Tanaka* [8]. According to the paper, measured AM-AM and AM-PM data (using conventional method) for a very high power TWTA with a particular gain and output power were used to extract gain compression and phase variation data relative to small-signal gain and phase values. These secondary extracted values were used as the input information for the *HP EESOF Series IV* software simulation tool [8]. Once these data were entered and necessary test bench (software setup) were constructed with important parameter settings, simulation was run at 1 GHz carrier frequency to model the nonlinear behavior of the TWTA. Basically, this was just a simulation of any nonlinear device using UTTS method. In this thesis, no prior AM-AM and AM-PM data were

available for the solid-state amplifiers used for experimentation. The UTTS method was used to actually test a nonlinear device. The goal was to drive the Class A and Class C amplifier with an RF signal at 1 GHz having both amplitude and phase modulation and then figure out the AM to AM compression and AM to PM conversion factors using carrier and sideband power levels both at the input and output. Tests were conducted in the laboratory using RF signal generators, pre-amplifiers and power measurements were taken from the spectrum analyzer display grid. The input carrier power was varied from –23 dBm to +23 dBm. While doing this, the difference between the carrier level and the sideband with higher power level (the upper sideband) was kept between 10 to 11 dB. On the other hand, the difference between the upper and lower sidebands was maintained between 10 to 16 dB. These differences between carrier and sideband power levels were chosen to ensure three unequal spectrum components of the RF signal. Varying the AM and FM indices in the FLUKE 6060B Synthesized RF Signal Generator, one can increase or decrease the relative differences between carrier and sideband power levels. Calculations of different parameters were based on input and output power levels of the carrier signal and sidebands. A set of quadratic equations, 14a and 14b relate these power levels to the AM-AM compression factor and AM-PM conversion coefficient of the nonlinear device under test. Due to high degree of linearity exhibited in small signal amplifiers (such as Class A), the AM-PM conversion coefficient are typically far less than 0.1°/dB when low level input signals are applied. As a result, the measurement of AM-PM conversion coefficient becomes extremely hard to measure [10]. For this reason, most manufactures of RF low noise amplifiers do not list the AM-PM conversion coefficient as a parameter on the device data sheet. But when a conversion coefficient Class A amplifier is driven into saturation and higher input levels are

applied, AM-PM can be considerably higher than 0.1°/dB. As the experimental results showed, the AM-PM conversion coefficient for a 10 dB gain Class A amplifier can be as high as 0.8 °/dB. According to data provided in Appendix A, the AM-PM conversion coefficient increases continuously with input power. For high power amplifiers, such as traveling wave tube amplifier (TWTA), the AM-PM conversion coefficient is usually higher than unity for low-level input power [8]. Using two unequal carrier signals (UB2T method) for deriving AM-PM conversion coefficient creates a complex measurement problem. In the case of a Class C amplifier, the results were consistent with our expectation. At every input power level, the bias point was adjusted manually for satisfactory Class C operation. In this case, when two low-level carrier signals are applied to the power amplifier under test, the resulting intermodulation products tend to be very near or below the amplifier noise floor. As a result, meaningful results are hard to obtain and sometimes cannot be reproduced without error [10]. In this thesis, the nonlinear RF characteristics of certain solid-state amplifiers have been investigated using UTTS method. These results were compared with AM-AM and AM-PM characteristics obtained from other solid-state amplifiers (Low Noise Amplifiers) & TWTA using traditional phase-bridge method and vector network analysis. The article by *Maurice J. Toolin* on *Microwave Technical Journal* and the IEEE short paper by *F.M. Ghannouchi, H. Wakana and M. Tanaka* include AM-AM and AM-PM characteristic curves for power amplifiers (both high power & small-signal) and TWTA. After careful observation, it can be concluded that the results in Appendix A correlate well with the AM-AM and AM-PM curves included in the above stated technical journals.

APPENDIX A. POWER AMPLIFIER DATA

Input Level (c) dBm (sa)	Input Level (c) volts (sa)	Output Level (c) dBm (sa)	Output Level (c) volts (sa)	Gain G, dB	Gain G, (v/v)
-20.43	0.030095392	-13.56	0.066374307	6.87	2.205464136
-19.43	0.033767585	-11.63	0.082889592	7.8	2.454708916
-18.43	0.037887853	-10.03	0.099655208	8.4	2.630267992
-17.43	0.042510871	-8.58	0.117760597	8.85	2.770129039
-16.43	0.047697981	-7.29	0.136615508	9.14	2.86417797
-15.23	0.05476461	-5.82	0.161808004	9.41	2.954608888
-14.23	0.061446903	-4.69	0.184289249	9.54	2.999162519
-13.27	0.068627788	-3.6	0.208929613	9.67	3.04438799
-12.32	0.076559661	-2.54	0.236047823	9.78	3.08318795
-11.34	0.085703785	-1.48	0.266685866	9.86	3.111716337
-10.36	0.095940063	-0.45	0.300261742	9.91	3.129680472
-9.2	0.10964782	0.77	0.34554133	9.97	3.15137438
-7.32	0.136144468	2.71	0.432016168	10.03	3.173218664
-6.34	0.152405275	3.71	0.484730113	10.05	3.180533688
-5.38	0.170215851	4.69	0.542625251	10.07	3.187865576
-4.4	0.190546072	5.68	0.608135001	10.08	3.191537855
-3.23	0.21802184	6.85	0.695824955	10.08	3.191537855
-2.28	0.243220401	7.79	0.775353943	10.07	3.187865576
-1.34	0.271019163	8.73	0.863972661	10.07	3.187865576
-0.38	0.302691343	9.67	0.962720013	10.05	3.180533688
0.6	0.338844156	10.61	1.072753648	10.01	3.165920463
1.55	0.378007137	11.5	1.188502227	9.95	3.14412642
2.7	0.431519077	12.5	1.333521432	9.8	3.090295433
3.61	0.479181453	13.23	1.450440774	9.62	3.026913428
4.55	0.533949274	13.92	1.570362804	9.37	2.941033694
6.42	0.662216504	15.12	1.803017741	8.7	2.722701308
8.68	0.859013522	16.36	2.079696687	7.68	2.421029047
9.53	0.947327185	16.76	2.177709772	7.23	2.298793709
10.39	1.04592369	17.16	2.280342072	6.77	2.180218397
11.2	1.148153621	17.51	2.374105423	6.31	2.067759382
12.02	1.261827535	17.85	2.468880105	5.83	1.956590768
12.8	1.380384265	18.16	2.558585887	5.36	1.853531623
13.58	1.510080154	18.47	2.651551093	4.89	1.755900894
14.31	1.64247966	18.74	2.735268726	4.43	1.665328828
14.99	1.776233268	18.99	2.815140015	4	1.584893192
15.69	1.925307045	19.23	2.894009817	3.54	1.503141966
16.36	2.079696687	19.47	2.975089259	3.11	1.430539981
17.04	2.249054606	19.69	3.051406029	2.65	1.35675053
17.93	2.491724371	19.97	3.15137438	2.04	1.264736347
18.58	2.685344446	20.15	3.217362533	1.57	1.198119123
19.23	2.894009817	20.3	3.273406949	1.07	1.131097389
19.89	3.122482406	20.4	3.311311215	0.51	1.060473938
20.56	3.372873087	20.45	3.330427623	-0.11	0.987415636
20.88	3.49945167	20.46	3.334264128	-0.42	0.952796164

Input Level (c) dBm (sa)	Output Level (c) dBm (sa)	Input USB Level dBm (sa)	Input USB Level volts (sa)	Input LSB Level dBm (sa)	Input LSB Level volts (sa)
-20.43	-13.56	-30	0.01	-40.5	0.002985383
-19.43	-11.63	-29	0.011220185	-40	0.003162278
-18.43	-10.03	-28	0.012589254	-39	0.003548134
-17.43	-8.58	-27	0.014125375	-38	0.003981072
-16.43	-7.29	-26	0.015848932	-37	0.004466836
-15.23	-5.82	-25	0.017782794	-36	0.005011872
-14.23	-4.69	-24	0.019952623	-35	0.005623413
-13.27	-3.6	-23	0.022387211	-34	0.006309573
-12.32	-2.54	-22	0.025118864	-33	0.007079458
-11.34	-1.48	-21	0.028183829	-32	0.007943282
-10.36	-0.45	-20	0.031622777	-31.5	0.008413951
-9.2	0.77	-19	0.035481339	-30	0.01
-7.32	2.71	-17	0.044668359	-28	0.012589254
-6.34	3.71	-16	0.050118723	-27.5	0.013335214
-5.38	4.69	-15	0.056234133	-26	0.015848932
-4.4	5.68	-14	0.063095734	-25.5	0.01678804
-3.23	6.85	-13	0.070794578	-24	0.019952623
-2.28	7.79	-12	0.079432823	-23.5	0.02113489
-1.34	8.73	-11	0.089125094	-22	0.025118864
-0.38	9.67	-10	0.1	-21.5	0.026607251
0.6	10.61	-9.5	0.105925373	-21	0.028183829
1.55	11.5	-8	0.125892541	-20	0.031622777
2.7	12.5	-7.5	0.133352143	-19	0.035481339
3.61	13.23	-6	0.158489319	-18	0.039810717
4.55	13.92	-5.5	0.167880402	-17	0.044668359
6.42	15.12	-4	0.199526231	-15.5	0.053088444
8.68	16.36	-2	0.251188643	-14	0.063095734
9.53	16.76	-1	0.281838293	-13.5	0.066834392
10.39	17.16	0	0.316227766	-13	0.070794578
11.2	17.51	0.5	0.334965439	-12.5	0.074989421
12.02	17.85	1	0.354813389	-12	0.079432823
12.8	18.16	2	0.398107171	-12	0.079432823
13.58	18.47	2	0.398107171	-12	0.079432823
14.31	18.74	2.5	0.421696503	-12	0.079432823
14.99	18.99	3	0.446683592	-12	0.079432823
15.69	19.23	4	0.501187234	-12	0.079432823
16.36	19.47	4	0.501187234	-11.5	0.084139514
17.04	19.69	4.5	0.530884444	-11	0.089125094
17.93	19.97	5	0.562341325	-8	0.125892541
18.58	20.15	6	0.630957344	-8	0.125892541
19.23	20.3	6.5	0.668343918	-7.5	0.133352143
19.89	20.4	7	0.707945784	-7	0.141253754
20.56	20.45	8	0.794328235	-6	0.158489319
20.88	20.46	8	0.794328235	-6	0.158489319

Input Level (c) dBm (sa)	Output Level (c) dBm (sa)	Output USB Level dBm (sa)	Output USB Level volts (sa)	Output LSB Level dBm (sa)	Output LSB Level volts (sa)
-20.43	-13.56	-20	0.031622777	-32	0.007943282
-19.43	-11.63	-19.5	0.033496544	-31	0.008912509
-18.43	-10.03	-18	0.039810717	-30	0.01
-17.43	-8.58	-17.5	0.04216965	-29	0.011220185
-16.43	-7.29	-16	0.050118723	-28	0.012589254
-15.23	-5.82	-15.5	0.053088444	-27	0.014125375
-14.23	-4.69	-14	0.063095734	-26	0.015848932
-13.27	-3.6	-13.5	0.066834392	-25	0.017782794
-12.32	-2.54	-12	0.079432823	-24	0.019952623
-11.34	-1.48	-11.5	0.084139514	-23	0.022387211
-10.36	-0.45	-11	0.089125094	-22	0.025118864
-9.2	0.77	-9.5	0.105925373	-21	0.028183829
-7.32	2.71	-7.5	0.133352143	-19	0.035481339
-6.34	3.71	-7	0.141253754	-18	0.039810717
-5.38	4.69	-6	0.158489319	-17	0.044668359
-4.4	5.68	-5	0.177827941	-16	0.050118723
-3.23	6.85	-4	0.199526231	-15	0.056234133
-2.28	7.79	-3	0.223872114	-14	0.063095734
-1.34	8.73	-2	0.251188643	-13	0.070794578
-0.38	9.67	-1	0.281838293	-12	0.079432823
0.6	10.61	0	0.316227766	-12.5	0.074989421
1.55	11.5	0.5	0.334965439	-11	0.089125094
2.7	12.5	1.5	0.375837404	-10	0.1
3.61	13.23	2	0.398107171	-10	0.1
4.55	13.92	2.5	0.421696503	-10	0.1
6.42	15.12	3.5	0.473151259	-12.5	0.074989421
8.68	16.36	4	0.501187234	-14	0.063095734
9.53	16.76	4	0.501187234	-12	0.079432823
10.39	17.16	4	0.501187234	-10	0.1
11.2	17.51	4	0.501187234	-8	0.125892541
12.02	17.85	4	0.501187234	-6	0.158489319
12.8	18.16	4	0.501187234	-5	0.177827941
13.58	18.47	4	0.501187234	-3	0.223872114
14.31	18.74	4.25	0.515822165	-2	0.251188643
14.99	18.99	4.25	0.515822165	-1.75	0.258523484
15.69	19.23	4.5	0.530884444	-1	0.281838293
16.36	19.47	4.5	0.530884444	-0.5	0.298538262
17.04	19.69	5	0.562341325	0	0.316227766
17.93	19.97	5.5	0.595662144	0.5	0.334965439
18.58	20.15	5.5	0.595662144	1	0.354813389
19.23	20.3	5.5	0.595662144	1.5	0.375837404
19.89	20.4	6	0.630957344	2	0.398107171
20.56	20.45	6	0.630957344	2	0.398107171
20.88	20.46	5.5	0.595662144	2	0.398107171

Input Level (c) dBm (sa)	Output Level (c) dBm (sa)	delta(USB-LSB) dB(input)	delta(USB-LSB) dB(output)	AM Index alpha	FM Index beta
-20.43	-13.56	10.5	12	0.431474119	0.233079451
-19.43	-11.63	11	11.5	0.425925107	0.238628463
-18.43	-10.03	11	12	0.425925107	0.238628463
-17.43	-8.58	11	11.5	0.425925107	0.238628463
-16.43	-7.29	11	12	0.425925107	0.238628463
-15.23	-5.82	11	11.5	0.416229868	0.233196616
-14.23	-4.69	11	12	0.416229868	0.233196616
-13.27	-3.6	11	11.5	0.418151098	0.234273003
-12.32	-2.54	11	12	0.420565111	0.235625476
-11.34	-1.48	11	11.5	0.421534613	0.236168649
-10.36	-0.45	11.5	11	0.417309794	0.24190963
-9.2	0.77	11	11.5	0.414794741	0.232392573
-7.32	2.71	11	11.5	0.420565111	0.235625476
-6.34	3.71	11.5	11	0.416350008	0.241353253
-5.38	4.69	11	11	0.423480329	0.237258753
-4.4	5.68	11.5	11	0.419236009	0.243026234
-3.23	6.85	11	11	0.416229868	0.233196616
-2.28	7.79	11.5	11	0.413483875	0.239691789
-1.34	8.73	11	11	0.421534613	0.236168649
-0.38	9.67	11.5	11	0.418271793	0.242467289
0.6	10.61	11.5	12.5	0.395784314	0.22943156
1.55	11.5	12	11.5	0.416699322	0.249386203
2.7	12.5	11.5	11.5	0.391253808	0.226805278
3.61	13.23	12	12	0.413830784	0.24766944
4.55	13.92	11.5	12.5	0.398069202	0.230756082
6.42	15.12	11.5	16	0.381468409	0.221132796
8.68	16.36	12	18	0.365866625	0.218963851
9.53	16.76	12.5	16	0.36805941	0.226958441
10.39	17.16	13	14	0.370029236	0.234656878
11.2	17.51	13	12	0.357055757	0.226429646
12.02	17.85	13	10	0.344140701	0.218239465
12.8	18.16	14	9	0.345947144	0.230859157
13.58	18.47	14	7	0.316234865	0.211031412
14.31	18.74	14.5	6.25	0.305105347	0.208382294
14.99	18.99	15	6	0.296197816	0.206758186
15.69	19.23	16	5.5	0.301572707	0.219058259
16.36	19.47	15.5	5	0.281448132	0.200532954
17.04	19.69	15.5	5	0.275675627	0.19642002
17.93	19.97	13	5	0.276207864	0.175159335
18.58	20.15	14	4.5	0.28184462	0.188081944
19.23	20.3	14	4	0.277019123	0.184861769
19.89	20.4	14	4	0.271962954	0.181487661
20.56	20.45	14	4	0.282494339	0.188515518
20.88	20.46	14	3.5	0.272276243	0.181696727

Input Level (c) dBm (sa)	Output Level (c) dBm (sa)	x1 center	x2 center	R1 radius	R2 radius
-20.43	-13.56	1.540193353	0.459806647	2.20838732	0.554721814
-19.43	-11.63	1.560259208	0.439740792	1.897565406	0.504889983
-18.43	-10.03	1.560259208	0.439740792	1.875844155	0.471190748
-17.43	-8.58	1.560259208	0.439740792	1.681499546	0.447400798
-16.43	-7.29	1.560259208	0.439740792	1.722648833	0.432709823
-15.23	-5.82	1.560259208	0.439740792	1.576510089	0.41946599
-14.23	-4.69	1.560259208	0.439740792	1.645116864	0.413234673
-13.27	-3.6	1.560259208	0.439740792	1.530018754	0.407095924
-12.32	-2.54	1.560259208	0.439740792	1.600282862	0.401972881
-11.34	-1.48	1.560259208	0.439740792	1.496913669	0.398287571
-10.36	-0.45	1.57968836	0.42031164	1.422562702	0.400932644
-9.2	0.77	1.560259208	0.439740792	1.478075963	0.393275375
-7.32	2.71	1.560259208	0.439740792	1.467900959	0.390568087
-6.34	3.71	1.57968836	0.42031164	1.399817498	0.394522174
-5.38	4.69	1.560259208	0.439740792	1.379420749	0.388773589
-4.4	5.68	1.57968836	0.42031164	1.394991039	0.393161893
-3.23	6.85	1.560259208	0.439740792	1.377833546	0.388326255
-2.28	7.79	1.57968836	0.42031164	1.396598007	0.393614798
-1.34	8.73	1.560259208	0.439740792	1.379420749	0.388773589
-0.38	9.67	1.57968836	0.42031164	1.399817498	0.394522174
0.6	10.61	1.57968836	0.42031164	1.489606017	0.353241254
1.55	11.5	1.598479982	0.401520018	1.352717791	0.359921013
2.7	12.5	1.57968836	0.42031164	1.440692907	0.383328772
3.61	13.23	1.598479982	0.401520018	1.32649984	0.333201695
4.55	13.92	1.57968836	0.42031164	1.349184732	0.31994212
6.42	15.12	1.57968836	0.42031164	1.375851045	0.218057695
8.68	16.36	1.598479982	0.401520018	1.317368279	0.16584684
9.53	16.76	1.616635345	0.383364655	1.250581701	0.198203842
10.39	17.16	1.634157668	0.365842332	1.187938496	0.237024891
11.2	17.51	1.634157668	0.365842332	1.182480415	0.297025651
12.02	17.85	1.634157668	0.365842332	1.179760785	0.373073117
12.8	18.16	1.667324938	0.332675062	1.132453155	0.401809542
13.58	18.47	1.667324938	0.332675062	1.195419253	0.533974166
14.31	18.74	1.682984734	0.317015266	1.236175627	0.601977386
14.99	18.99	1.698040886	0.301959114	1.23722345	0.620080598
15.69	19.23	1.726386223	0.273613777	1.216572406	0.645859365
16.36	19.47	1.71250412	0.28749588	1.268036121	0.713069113
17.04	19.69	1.71250412	0.28749588	1.33700067	0.751850729
17.93	19.97	1.634157668	0.365842332	1.368654899	0.76965121
18.58	20.15	1.667324938	0.332675062	1.313772739	0.782564686
19.23	20.3	1.667324938	0.332675062	1.313772739	0.828934559
19.89	20.4	1.667324938	0.332675062	1.401264908	0.884138385
20.56	20.45	1.667324938	0.332675062	1.341282462	0.84629202
20.88	20.46	1.667324938	0.332675062	1.312261073	0.877041706

Input Level (c) dBm (sa)	Output Level (c) dBm (sa)	AM-AM C	AM-AM C, %	AM-PM Kp, degree/dB	Peak Phase Change delta(theta), degree
-20.43	-13.56	0	0	0	0
-19.43	-11.63	0	0	0	0
-18.43	-10.03	0	0	0	0
-17.43	-8.58	0	0	0	0
-16.43	-7.29	0	0	0	0
-15.23	-5.82	0	0	0	0
-14.23	-4.69	0	0	0	0
-13.27	-3.6	0	0	0	0
-12.32	-2.54	0	0	0	0
-11.34	-1.48	0.070913287	7.091328677	0.150330505	0.063369511
-10.36	-0.45	0.076577943	7.657794285	0.227013939	0.09473514
-9.2	0.77	0.084150082	8.415008206	0.287703442	0.119337875
-7.32	2.71	0.086578809	8.657880888	0.293829643	0.123574496
-6.34	3.71	0.092064213	9.206421283	0.30109486	0.125360847
-5.38	4.69	0.098372195	9.837219541	0.319594819	0.135342119
-4.4	5.68	0.107419485	10.74194851	0.322591434	0.135241945
-3.23	6.85	0.110169889	11.01698895	0.330290335	0.137476703
-2.28	7.79	0.125638503	12.56385031	0.342103755	0.141454386
-1.34	8.73	0.128372195	12.83721954	0.359594819	0.151581663
-0.38	9.67	0.142064213	14.20642128	0.36109486	0.151035794
0.6	10.61	0.152865295	15.28652949	0.371992412	0.147228762
1.55	11.5	0.160741371	16.07413708	0.382123763	0.159230713
2.7	12.5	0.178236229	17.82362289	0.388788737	0.152115074
3.61	13.23	0.182347704	18.23477037	0.390768333	0.161711965
4.55	13.92	0.20911205	20.911205	0.403650702	0.160680913
6.42	15.12	0.254134037	25.41340368	0.417275284	0.159177339
8.68	16.36	0.316545056	31.65450558	0.419523774	0.153489747
9.53	16.76	0.381859214	38.18592137	0.428198125	0.157602349
10.39	17.16	0.465820119	46.58201189	0.434907518	0.160928497
11.2	17.51	0.483552845	48.35528454	0.442705835	0.158070667
12.02	17.85	0.506174875	50.61748752	0.445673731	0.15337447
12.8	18.16	0.540039957	54.00399567	0.46664099	0.161433118
13.58	18.47	0.5714611	57.14611002	0.477608247	0.15103638
14.31	18.74	0.593287165	59.32871652	0.544703118	0.166191834
14.99	18.99	0.60948611	60.94861099	0.549388911	0.162727796
15.69	19.23	0.634177362	63.41773616	0.535843467	0.161595765
16.36	19.47	0.644230987	64.42309868	0.633807328	0.178383889
17.04	19.69	0.665128349	66.51283487	0.696298888	0.191952632
17.93	19.97	0.685057258	68.5057258	0.758726886	0.209566333
18.58	20.15	0.702815185	70.28151855	0.774321092	0.218238234
19.23	20.3	0.710809424	71.08094244	0.780880131	0.216318729
19.89	20.4	0.737246182	73.72461818	0.855142384	0.232567049
20.56	20.45	0.75433988	75.43398797	0.804824022	0.22735823
20.88	20.46	0.773042349	77.30423494	0.820289157	0.22334525

Note :

The above data pertains to Class A power amplifier circuit that was used in our experiment.

'c' refers to the carrier components of both input and output signal.

'sa' refers to the measurements recorded from spectrum analyzer.

Input Level (c) dBm (sa)	Input Level (c) volts (sa)	Output Level (c) dBm (sa)	Output Level (c) volts (sa)	G ain G, dB	Gain G, (v/v)
-20	0.031622777	-12	0.079432823	8	2.511886432
-19	0.035481339	-11	0.089125094	8	2.511886432
-18	0.039810717	-10	0.1	8	2.511886432
-17	0.044668359	-9	0.112201845	8	2.511886432
-16	0.050118723	-8	0.125892541	8	2.511886432
-15	0.056234133	-7	0.141253754	8	2.511886432
-14	0.063095734	-6	0.158489319	8	2.511886432
-13	0.070794578	-5	0.177827941	8	2.511886432
-12	0.079432823	-4	0.199526231	8	2.511886432
-11	0.089125094	-4	0.199526231	7	2.238721139
-10	0.1	-2.45	0.23850638	7.55	2.385063795
-9	0.112201845	-1.3	0.272270131	7.7	2.426610095
-8	0.125892541	-0.1	0.312607937	7.9	2.483133105
-7	0.141253754	1.3	0.3672823	8.3	2.600159563
-6	0.158489319	2.52	0.422668614	8.52	2.666858665
-5	0.177827941	3.73	0.485847531	8.73	2.732121444
-4	0.199526231	4.85	0.552713408	8.85	2.770129039
-3	0.223872114	6	0.630957344	9	2.818382931
-2	0.251188643	7.18	0.722769804	9.18	2.877398415
-1	0.281838293	8.23	0.815642787	9.23	2.894009817
0	0.316227766	9.31	0.923634188	9.31	2.92078776
1	0.354813389	10.47	1.055601503	9.47	2.975089259
2	0.398107171	11.65	1.209205183	9.65	3.037386092
3	0.446683592	13.1	1.428893959	10.1	3.19889511
4	0.501187234	14.5	1.678804018	10.5	3.349654392
5	0.562341325	16.5	2.11348904	11.5	3.758374043
6	0.630957344	16.3	2.065380156	10.3	3.273406949
7	0.707945784	16.8	2.187761624	9.8	3.090295433
8	0.794328235	17	2.238721139	9	2.818382931
9	0.891250938	17.3	2.31739465	8.3	2.600159563
10	1	18	2.511886432	8	2.511886432
11	1.122018454	18	2.511886432	7	2.238721139
12	1.258925412	18.5	2.66072506	6.5	2.11348904
13	1.412537545	19	2.818382931	6	1.995262315
14	1.584893192	19	2.818382931	5	1.77827941
15	1.77827941	19.44	2.96483139	4.44	1.667247213
16	1.995262315	20	3.16227766	4	1.584893192
17	2.238721139	20	3.16227766	3	1.412537545
18	2.511886432	20	3.16227766	2	1.258925412
19	2.818382931	20	3.16227766	1	1.122018454

Input Level (c) dBm (sa)	Output Level (c) dBm (sa)	Input USB Level dBm (sa)	Input USB Level volts (sa)	Input LSB Level dBm (sa)	Input LSB Level volts (sa)
-20	-12	-29	0.011220185	-39	0.003548134
-19	-11	-28	0.012589254	-38	0.003981072
-18	-10	-27	0.014125375	-37	0.004466836
-17	-9	-26	0.015848932	-36	0.005011872
-16	-8	-25	0.017782794	-35	0.005623413
-15	-7	-24	0.019952623	-34	0.006309573
-14	-6	-23	0.022387211	-33	0.007079458
-13	-5	-22	0.025118864	-32	0.007943282
-12	-4	-21	0.028183829	-31	0.008912509
-11	-4	-20	0.031622777	-30	0.01
-10	-2.45	-19	0.035481339	-29	0.011220185
-9	-1.3	-18	0.039810717	-28	0.012589254
-8	-0.1	-17	0.044668359	-27	0.014125375
-7	1.3	-16	0.050118723	-26	0.015848932
-6	2.52	-15	0.056234133	-25	0.017782794
-5	3.73	-14	0.063095734	-24	0.019952623
-4	4.85	-13	0.070794578	-23	0.022387211
-3	6	-12	0.079432823	-22	0.025118864
-2	7.18	-11	0.089125094	-21	0.028183829
-1	8.23	-10	0.1	-20	0.031622777
0	9.31	-9	0.112201845	-19	0.035481339
1	10.47	-8	0.125892541	-18	0.039810717
2	11.65	-7	0.141253754	-17	0.044668359
3	13.1	-6	0.158489319	-16	0.050118723
4	14.5	-5	0.177827941	-15	0.056234133
5	16.5	-4	0.199526231	-14	0.063095734
6	16.3	-3	0.223872114	-13	0.070794578
7	16.8	-2	0.251188643	-12	0.079432823
8	17	-1	0.281838293	-11	0.089125094
9	17.3	0	0.316227766	-10	0.1
10	18	1	0.354813389	-9	0.112201845
11	18	2	0.398107171	-8	0.125892541
12	18.5	3	0.446683592	-7	0.141253754
13	19	4	0.501187234	-6	0.158489319
14	19	5	0.562341325	-5	0.177827941
15	19.44	6	0.630957344	-4	0.199526231
16	20	7	0.707945784	-3	0.223872114
17	20	8	0.794328235	-2	0.251188643
18	20	9	0.891250938	-1	0.281838293
19	20	10	1	0	0.316227766

Input Level (c) dBm (sa)	Output Level (c) dBm (sa)	Output USB Level dBm (sa)	Output USB Level volts (sa)	Output LSB Level dBm (sa)	Output LSB Level volts (sa)
-20	-12	-20	0.031622777	-31	0.008912509
-19	-11	-19	0.035481339	-30	0.01
-18	-10	-18	0.039810717	-29	0.011220185
-17	-9	-17	0.044668359	-28	0.012589254
-16	-8	-16	0.050118723	-27	0.014125375
-15	-7	-15	0.056234133	-26	0.015848932
-14	-6	-14	0.063095734	-25	0.017782794
-13	-5	-13	0.070794578	-24	0.019952623
-12	-4	-12	0.079432823	-23	0.022387211
-11	-4	-11	0.089125094	-22	0.025118864
-10	-2.45	-10	0.1	-21	0.028183829
-9	-1.3	-9	0.112201845	-20	0.031622777
-8	-0.1	-8	0.125892541	-19	0.035481339
-7	1.3	-7	0.141253754	-18	0.039810717
-6	2.52	-6	0.158489319	-17	0.044668359
-5	3.73	-5	0.177827941	-16	0.050118723
-4	4.85	-4	0.199526231	-15	0.056234133
-3	6	-3	0.223872114	-14	0.063095734
-2	7.18	-2	0.251188643	-13	0.070794578
-1	8.23	-1	0.281838293	-12	0.079432823
0	9.31	2	0.398107171	-11	0.089125094
1	10.47	5	0.562341325	-8	0.125892541
2	11.65	4	0.501187234	-8	0.125892541
3	13.1	5	0.562341325	-7	0.141253754
4	14.5	5	0.562341325	-7	0.141253754
5	16.5	6	0.630957344	-8	0.125892541
6	16.3	6	0.630957344	-10	0.1
7	16.8	6	0.630957344	-12	0.079432823
8	17	6	0.630957344	-15	0.056234133
9	17.3	6	0.630957344	-15	0.056234133
10	18	6	0.630957344	-13	0.070794578
11	18	6	0.630957344	-9	0.112201845
12	18.5	6	0.630957344	-5	0.177827941
13	19	6	0.630957344	-2	0.251188643
14	19	7	0.707945784	1	0.354813389
15	19.44	7	0.707945784	3	0.446683592
16	20	7	0.707945784	3	0.446683592
17	20	6	0.630957344	2	0.398107171
18	20	6	0.630957344	1	0.354813389
19	20	4	0.501187234	0	0.316227766

Input Level (c) dBm (sa)	Output Level (c) dBm (sa)	USB-LSB_Level at Input, dB	USB-LSB_Level at Output, dB	AM Index alpha	FM Index beta
-20	-12	10	11	0.467015235	0.242611544
-19	-11	10	11	0.467015235	0.242611544
-18	-10	10	11	0.467015235	0.242611544
-17	-9	10	11	0.467015235	0.242611544
-16	-8	10	11	0.467015235	0.242611544
-15	-7	10	11	0.467015235	0.242611544
-14	-6	10	11	0.467015235	0.242611544
-13	-5	10	11	0.467015235	0.242611544
-12	-4	10	11	0.467015235	0.242611544
-11	-4	10	11	0.467015235	0.242611544
-10	-2.45	10	11	0.467015235	0.242611544
-9	-1.3	10	11	0.467015235	0.242611544
-8	-0.1	10	11	0.467015235	0.242611544
-7	1.3	10	11	0.467015235	0.242611544
-6	2.52	10	11	0.467015235	0.242611544
-5	3.73	10	11	0.467015235	0.242611544
-4	4.85	10	11	0.467015235	0.242611544
-3	6	10	11	0.467015235	0.242611544
-2	7.18	10	11	0.467015235	0.242611544
-1	8.23	10	11	0.467015235	0.242611544
0	9.31	10	13	0.467015235	0.242611544
1	10.47	10	13	0.467015235	0.242611544
2	11.65	10	12	0.467015235	0.242611544
3	13.1	10	12	0.467015235	0.242611544
4	14.5	10	12	0.467015235	0.242611544
5	16.5	10	14	0.467015235	0.242611544
6	16.3	10	16	0.467015235	0.242611544
7	16.8	10	18	0.467015235	0.242611544
8	17	10	21	0.467015235	0.242611544
9	17.3	10	21	0.467015235	0.242611544
10	18	10	19	0.467015235	0.242611544
11	18	10	15	0.467015235	0.242611544
12	18.5	10	11	0.467015235	0.242611544
13	19	10	8	0.467015235	0.242611544
14	19	10	6	0.467015235	0.242611544
15	19.44	10	4	0.467015235	0.242611544
16	20	10	4	0.467015235	0.242611544
17	20	10	4	0.467015235	0.242611544
18	20	10	5	0.467015235	0.242611544
19	20	10	4	0.467015235	0.242611544

Input Level (c) dBm (sa)	Output Level (c) dBm (sa)	x1 center	x2 center	R1 radius	R2 radius
-20	-12	1.519493853	0.480506147	1.704900145	0.480506147
-19	-11	1.519493853	0.480506147	1.704900145	0.480506147
-18	-10	1.519493853	0.480506147	1.704900145	0.480506147
-17	-9	1.519493853	0.480506147	1.704900145	0.480506147
-16	-8	1.519493853	0.480506147	1.704900145	0.480506147
-15	-7	1.519493853	0.480506147	1.704900145	0.480506147
-14	-6	1.519493853	0.480506147	1.704900145	0.480506147
-13	-5	1.519493853	0.480506147	1.704900145	0.480506147
-12	-4	1.519493853	0.480506147	1.704900145	0.480506147
-11	-4	1.519493853	0.480506147	1.704900145	0.480506147
-10	-2.45	1.519493853	0.480506147	1.704900145	0.480506147
-9	-1.3	1.519493853	0.480506147	1.704900145	0.480506147
-8	-0.1	1.519493853	0.480506147	1.704900145	0.480506147
-7	1.3	1.519493853	0.480506147	1.704900145	0.480506147
-6	2.52	1.519493853	0.480506147	1.704900145	0.480506147
-5	3.73	1.519493853	0.480506147	1.704900145	0.480506147
-4	4.85	1.519493853	0.480506147	1.704900145	0.480506147
-3	6	1.519493853	0.480506147	1.704900145	0.480506147
-2	7.18	1.519493853	0.480506147	1.704900145	0.480506147
-1	8.23	1.519493853	0.480506147	1.704900145	0.480506147
0	9.31	1.519493853	0.480506147	1.704900145	0.381679599
1	10.47	1.519493853	0.480506147	2.146342117	0.480506147
2	11.65	1.519493853	0.480506147	1.704900145	0.428251554
3	13.1	1.519493853	0.480506147	1.704900145	0.428251554
4	14.5	1.519493853	0.480506147	1.519493853	0.381679599
5	16.5	1.519493853	0.480506147	1.519493853	0.303178882
6	16.3	1.519493853	0.480506147	1.354250322	0.214634212
7	16.8	1.519493853	0.480506147	1.354250322	0.170490014
8	17	1.519493853	0.480506147	1.20697687	0.107571927
9	17.3	1.519493853	0.480506147	1.20697687	0.107571927
10	18	1.519493853	0.480506147	1.075719268	0.120697687
11	18	1.519493853	0.480506147	1.075719268	0.191292942
12	18.5	1.519493853	0.480506147	1.075719268	0.303178882
13	19	1.519493853	0.480506147	0.958735807	0.381679599
14	19	1.519493853	0.480506147	1.075719268	0.539136764
15	19.44	1.519493853	0.480506147	1.075719268	0.678732973
16	20	1.519493853	0.480506147	0.958735807	0.604921399
17	20	1.519493853	0.480506147	0.854474187	0.539136764
18	20	1.519493853	0.480506147	0.854474187	0.480506147
19	20	1.519493853	0.480506147	0.678732973	0.428251554

Input Level (c)	Output Level (c)	AM-AM	AM-AM	AM-PM	Peak Phase Change
dBm (sa)	dBm (sa)	C	C, %	Kp , degree/dB	delta(theta), degree
-20	-12	0	0	0	0
-19	-11	0	0	0	0
-18	-10	0	0	0	0
-17	-9	0	0	0	0
-16	-8	0	0	0	0
-15	-7	0	0	0	0
-14	-6	0	0	0	0
-13	-5	0	0	0	0
-12	-4	0	0	0	0
-11	-4	0	0	0	0
-10	-2.45	0	0	0	0
-9	-1.3	0	0	0	0
-8	-0.1	0	0	0	0
-7	1.3	0	0	0	0
-6	2.52	0	0	0	0
-5	3.73	0	0	0	0
-4	4.85	0	0	0	0
-3	6	0	0	0	0
-2	7.18	0	0	0	0
-1	8.23	0	0	0	0
0	9.31	0	0	0	0
1	10.47	0	0	0	0
2	11.65	0	0	0	0
3	13.1	0	0	0	0
4	14.5	0	0	0	0
5	16.5	0	0	0	0
6	16.3	0.139582654	13.95826538	0	0
7	16.8	0.131401133	13.14011327	0	0
8	17	0.304505031	30.4505031	0	0
9	17.3	0.304505031	30.4505031	0	0
10	18	0.450135933	45.01359331	0.116814305	0.05455406
11	18	0.46073522	46.07352203	0.190268495	0.088858286
12	18.5	0.487359426	48.7359426	0.303101414	0.141552978
13	19	0.627765071	62.7765071	0.352127996	0.164449139
14	19	0.583005897	58.30058973	0.529303553	0.247192823
15	19.44	0.664821109	66.48211087	0.593227711	0.277046379
16	20	0.733757943	73.3757943	0.649357285	0.303259745
17	20	0.788516417	78.85164168	0.694249082	0.324224898
18	20	0.759746927	75.97469266	0.733803375	0.342697355
19	20	0.86656288	86.656288	0.775363406	0.362106523

Note :

The above data pertains to Class C power amplifier circuit that was used in our experiment.

'c' refers to the carrier components of both input and output signal.

'sa' refers to the measurements recorded from spectrum analyzer.

APPENDIX B. RF TRANSISTOR DATA

MOTOROLA
SEMICONDUCTOR TECHNICAL DATA

Order this document
by MMBR901LT1/D

The RF Line

NPN Silicon High-Frequency Transistor

MMBR901LT1, T3

I_C = 30 mA
SURFACE MOUNTED
HIGH-FREQUENCY
TRANSISTOR
NPN SILICON

Designed primarily for use in high–gain, low–noise small–signal amplifiers for operation up to 2.5 GHz. Also usable in applications requiring fast switching times.

- High Current–Gain — Bandwidth Product
- Low Noise Figure @ f = 1.0 GHz —
  $NF_{(matched)}$ = 1.9 dB (Typ)
- High Power Gain —
  $G_{pe(matched)}$ = 12.0 dB (Typ) @ f = 1.0 GHz
- Surface Mounted SOT–23 Offers Improved RF Performance, Lower Package Parasitics and High Gain
- Available in tape and reel packaging options:
  T1 suffix = 3,000 units per reel
  T3 suffix = 10,000 units per reel

CASE 318–08, STYLE 6
SOT–23

HOT RECOMMENDED FOR NEW DESIGNS:
PRODUCT TO BE PHASED OUT.

MAXIMUM RATINGS

Rating	Symbol	Value	Unit
Collector–Emitter Voltage	V_{CEO}	15	Vdc
Collector–Base Voltage	V_{CBO}	25	Vdc
Emitter–Base Voltage	V_{EBO}	2.0	Vdc
Collector Current — Continuous	I_C	30	mAdc
Power Dissipation @ T_C = 75°C (1) Derate above 75°C	$P_{D(max)}$	0.300 4.0	Watt mW/°C
Storage Temperature Range	T_{stg}	−55 to +150	°C
Maximum Junction Temperature	$T_{J(max)}$	150	°C

THERMAL CHARACTERISTICS

Characteristic	Symbol	Max	Unit
Storage Temperature	T_{stg}	150	°C
Thermal Resistance, Junction to Case	$R_{\theta JC}$	250	°C/W

DEVICE MARKING

MMBR901LT1, T3 = 7A

NOTE:
1. Case temperature measured on collector lead immediately adjacent to body of package.

ELECTRICAL CHARACTERISTICS (T_A = 25°C unless otherwise noted)

Characteristic	Symbol	Min	Typ	Max	Unit
OFF CHARACTERISTICS					
Collector–Emitter Breakdown Voltage (I_C = 1.0 mAdc, I_B = 0)	$V_{(BR)CEO}$	15	—	—	Vdc
Collector–Base Breakdown Voltage (I_C = 0.1 mAdc, I_E = 0)	$V_{(BR)CBO}$	25	—	—	Vdc
Emitter–Base Breakdown Voltage (I_E = 0.1 mAdc, I_C = 0)	$V_{(BR)EBO}$	2.0	—	—	Vdc
Collector Cutoff Current (V_{CB} = 15 Vdc, I_E = 0)	I_{CBO}	—	—	50	nAdc
ON CHARACTERISTICS					
DC Current Gain (I_C = 5.0 mAdc, V_{CE} = 5.0 Vdc)	h_{FE}	50	—	200	—
FUNCTIONAL TESTS					
Minimum Noise Figure (V_{CE} = 6.0 Vdc, I_C = 5.0 mA, f = 1.0 GHz) (V_{CE} = 10 Vdc, I_C = 5.0 mA, f = 1.0 GHz)	NF_{min}	—	1.9	—	dB
SMALL–SIGNAL CHARACTERISTICS					
Output Capacitance (V_{CB} = 10 Vdc, I_C = 5.0 mAdc, f = 1.0 GHz)	C_{obo}	—	—	1.0	pF
Common–Emitter Amplifier Gain (V_{CC} = 6.0 Vdc, I_C = 5.0 mAdc, f = 1.0 GHz)	G_{pe}	—	12	—	dB

PACKAGE DIMENSIONS

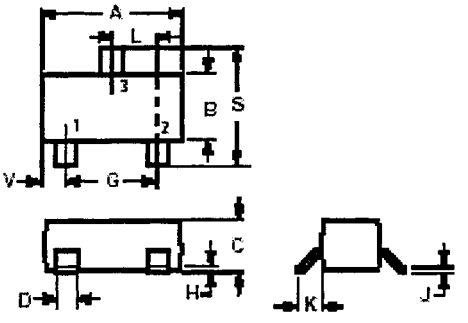

NOTES:
1. DIMENSIONING AND TOLERANCING PER ANSI Y14.5M, 1982.
2. CONTROLLING DIMENSION: INCH.
3. MAXIMUM LEAD THICKNESS INCLUDES LEAD FINISH THICKNESS. MINIMUM LEAD THICKNESS IS THE MINIMUM THICKNESS OF BASE MATERIAL.

DIM	INCHES MIN	INCHES MAX	MILLIMETERS MIN	MILLIMETERS MAX
A	0.1102	0.1197	2.80	3.04
B	0.0472	0.0551	1.20	1.40
C	0.0350	0.0440	0.89	1.11
D	0.0150	0.0200	0.37	0.50
G	0.0701	0.0807	1.78	2.04
H	0.0005	0.0040	0.013	0.100
J	0.0034	0.0070	0.085	0.177
K	0.0140	0.0285	0.35	0.69
L	0.0350	0.0401	0.89	1.02
S	0.0830	0.1039	2.10	2.64
V	0.0177	0.0236	0.45	0.60

STYLE 6:
PIN 1. BASE
2. EMITTER
3. COLLECTOR

CASE 318–08
ISSUE AF

BIBLIOGRAPHY

[1] Robert J. Weber, *Microwave Engineering Course Notes*, Version August 14, 1997.

[2] Guillermo Gonzalez, *Microwave Transistor Amplifiers : Analysis and Design, 2nd Edition*, Prentice-Hall, Inc., New Jersey, 1997.

[3] Reinhold Ludwig and Pavel Bretchko, *RF Circuit Design : Theory and Application,* Prentice-Hall, Inc., New Jersey, 2000.

[4] Herbert L. Krauss, Charles W. Bostian and Frederick H. Raab, *Solid State Radio Engineering*, John Wiley & Sons, Inc., New York, 1980.

[5] Adel S. Sedra and Kenneth C. Smith, *Microelectronics Circuits, 3rd Edition,* Saunders College Publishing, Harcourt Brace & Company, Orland, Florida 1991.

[6] Simon Haykin, *Communication Systems, 2nd Edition*, John Wiley & Sons, Inc., New York, 1984.

[7] Leon W. Couch II, *Digital and Analog Communication Systems, 5th Edition,* Prentice-Hall, Inc., New Jersey, 1997.

[8] F. M. Ghannouchi, H. Wakana, and M. Tanaka, "*A New Unequal Three-Tone Signal Method for AM-AM and AM-PM Distortion Measurements Suitable for Characterization of Satellite Communication Transmitters/Transponders,*" *IEEE Transactions On Microwave Theory And Techniques*, Vol. 48, No. 8, August 2000.

[9] J. P. Laico, "*A Medium Power TWT for 6000 MHz Radio Relay,*" *The Bell System Technical Journal*, Vol. 35, No. 6, November 1956.

[10] Maurice J. Toolin, "*A Simplified Approach To Determining AM/PM Conversion Coefficient in Microwave Low Noise Amplifiers and Systems*," *Microwave Journal*, August 2000.

[11] Ulrich L. Rohde and David P. Newkirk, *RF/Microwave Circuit Design for Wireless Applications,* John Wiley & Sons, Inc., New York, 2000.